Journal of Plant Physiology 306 (2025) 154453

Contents lists available at ScienceDirect

Journal of Plant Physiology

journal homepage: www.elsevier.com/locate/jplph

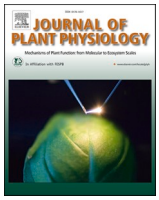

Reduction of the geomagnetic field to hypomagnetic field modulates tomato (*Solanum lycopersicum* L. cv Microtom) gene expression and metabolomics during plant development

Giuseppe Mannino, Ambra S. Parmagnani, Massimo E. Maffei *

Department of Life Sciences and Systems Biology, University of Turin, 10135, Turin, Italy

ARTICLE INFO

Keywords:
Hypomagnetic field
Gene expression
Flavonoids
Reactive oxygen species
Iron-sulfur cluster assembly
Fruit set
Plant hormones

ABSTRACT

An interesting aspect that links the geomagnetic field (GMF) to the evolution of life lies in how plants respond to the reduction of the GMF, also known as hypomagnetic field (HMF). In this work, tomato plants (*Solanum lycopersicum* cv Microtom) were exposed either to GMF or HMF and were studied during the development of leaves and fruit set. Changes of expression of genes encoding for primary and secondary metabolites, including Reactive Oxygen Species (ROS), proteins, fatty acids, polyphenols, chlorophylls, carotenoids and phytohormones were assessed by qRT-PCR, while the corresponding metabolite levels were quantified by GC-MS and HPLC-MS. Two tomato homologs of the fruit fly magnetoreceptor MagR, *Isca-like 1* and *erpA 2*, were modulated by HMF, as were numerous tomato genes under investigation. In tomato leaves, positive correlations were observed with most of the genes associated with phytohormones production, ROS scavenging and production, and lipid metabolism, whereas an almost reversed trend was found in flowers and fruits. Interestingly, downregulation of *Isca-like 1* and *erpA 2* was found to correlate with an upregulation of most unripe fruit genes. Exposure to HMF reduced chlorophyll and carotenoid content, decreased photosynthetic efficiency and increased non-photochemical quenching. Auxins, gibberellins, cytokinins, abscisic acid, jasmonic acid and salicylic acid content and the expression of genes related to their metabolism correlated with tomato ISCA modulation. The results here reported suggest that *Isca-like 1* and *erpA* 2 might be important players in tomato magnetoreception.

1. Introduction

The Earth magnetic field (or geomagnetic field, GMF) is a natural condition that was established long before the existence of any life form (Maffei, 2022). Therefore, all living organisms present on our planet evolved in the presence of the GMF. The ability of living organisms to respond to GMF variations, or magnetoperception, has been demonstrated only in migratory birds (Nießner et al., 2014), although magnetic induction is known also in plants (Maffei, 2022). Experiments on model plants and crops showed that reducing the GMF (~45 μT) to cosmic values (~20 nT) (also known as hypomagnetic field, HMF) delays plant transition to flowering (Agliassa et al., 2018a; Xu et al., 2013) and changes clock gene amplitude (Agliassa and Maffei, 2019) by altering photoreceptor signalling, in a light-independent manner (Agliassa et al., 2018b; Dhiman and Galland, 2018). Interestingly, by differentially regulating genes in shoot and roots, the GMF responses in Arabidopsis suggest that both organs are magnetoperceptive (Paponov et al., 2021). HMF also affects ROS production and photosynthetic activity in several plants species, including *Arabidopsis thaliana* (Parmagnani et al., 2022b; Pooam et al., 2019), maize (*Zea mays*) (Fiorillo et al., 2023) and Lima bean (*Phaseolus lunatus*) (Parmagnani et al., 2023). More recently, we showed that some *A. thaliana* iron-sulfur cluster assembly (ISCA) proteins which are homologs to *Drosophila melanogaster* magnetosensor (MagR) (Qin et al., 2016), are good potential candidates as plant magnetosensors (Parmagnani et al., 2022a). Besides Arabidopsis, this hypothesis was also tested on maize (Fiorillo et al., 2023) and Lima bean (Parmagnani et al., 2023), where the homologous of the MagR gene were found to be modulated by HMFs.

Tomato is a rich source for human nutrition owing to its contents of important phytonutrients, including minerals, vitamins, carotenoids and polyphenols (Yong et al., 2023). Besides nutrition, tomato phytoconstituents possess the potential to reduce human disease (Storniolo et al., 2020) and fight against reactive oxygen and nitrogen species (Fattore et al., 2016). Among tomato phytochemicals, lycopene, a carotenoid,

* Corresponding author.
E-mail address: massimo.maffei@unito.it (M.E. Maffei).

https://doi.org/10.1016/j.jplph.2025.154453
Received 25 September 2024; Received in revised form 14 February 2025; Accepted 14 February 2025
Available online 15 February 2025

acts as a potent antioxidant compound, with anti-aging actions that contribute to the mitigation of chronic disorders (Abir et al., 2023). Recently, also unripe tomato fruits gained a considerable attention due to the presence of bioactive compounds with interesting nutraceutical properties (Patel et al., 2023; Piccolo et al., 2024).

A survey of the literature indicates that tomato interacts with MFs. Exposure of tomato to MF intensities higher than the GMF (from 250 to 500 mT) showed the absence of morphological responses; however, proteomic analyses revealed differential expression of proteins involved in ethylene-responsive methionine synthase, dehydroquinate synthase, peroxidases and several proteins involved in primary metabolism (Villani et al., 2017). Increased MF also induced higher levels of tomato chlorophyll (Racuciu, 2019) and catalase activity (Yang et al., 2020), delayed fruit ripening and reduced the production of ethylene and the synthesis of lycopene (Kumar et al., 2014), enhanced water relations and photosynthesis (De Souza-Torres et al., 2020), reduced electrolyte leakage (Poinapen et al., 2013), promoted seed germination (Bourget et al., 2011) and increased fruit weight and the fruit yield per plant/area (de Souza et al., 2006). Several reports also relate to tomato responses to magnetized water treatments, with increased values of plant height, mineral nutrition, stem diameter, and fruit yield, on a per plant basis (Ageeb et al., 2018; Samarah et al., 2021). However, to our knowledge, no data are available on tomato responses to HMF.

The aim of this work is to assess whether the reduction of the GMF to HMF modulates tomato gene expression, with particular reference to two tomato ISCA homologs of the MagR gene. Here we show that reducing the GMF to HMF modulates MagR homologs and induces metabolic and gene expression changes in tomato developing plants.

2. Materials and methods

2.1. Plant material and growth conditions

Tomato plants *(Solanum lycopersicum* L. cv Microtom) were grown in plastic pots with sterilized peat soil at 22 °C (±1.5 °C) and 60% (v/v) humidity by using 120 μmol m^{-2} s^{-1} light provided by a tuneable LED lighting system source (PHYTOFY RL 150W, Osram, München, DE), using a photoperiod consisting of 16h light and 8h darkness. Before sowing, sterilization of seeds was obtained by soaking in 70% (v/v) ethanol for 10 min. Seeds were then rinsed in distilled water several times and then sawn using a standard soil for plant growth in pots.

2.2. Exposure of tomato to GMF and HMF conditions

The local GMF values where typical of the Northern hemisphere at 45°0′59″ N and 7°36′58″ E coordinates. Hypomagnetic field (HMF) was generated as previously described (Agliassa et al., 2018a). Real-time control of magnetic field was done by using a triaxial fluxgate (model Mag-03, Bartington Instruments, Oxford, U.K.) as recently reported (Parmagnani et al., 2023). Pots containing tomato plants were then exposed to HMF conditions. After an exposure period of 48 days after sawing (DAS) (flowering time), 75 DAS (unripe fruit stage) or 90 DAS (ripe fruit stage), leaves, flowers, and fruits were separately harvested. After sampling, samples were immediately frozen in liquid nitrogen and stored at −80 °C for further analysis. For each condition (GMF or HMF), three different biological replicates were always considered.

2.3. Chlorophyll a fluorescence kinetics

Chlorophyll fluorescence parameters Ft, QY, NPQ, and OJIP were obtained with a FP100 fluorometer (Photon Systems Instruments, Drásov, Czech Republic). Measurements were performed in triplicate by following the manufacturer instructions as previously reported (Parmagnani et al., 2023).

2.4. Total protein and H_2O_2 quantification

One hundred mg of fresh leaves, flowers or fruits was grinded in liquid nitrogen and then extracted with a buffer composed of 50 mM Na-P at pH 7. Quantification of total protein content was performed in triplicate and achieved using a Protein Assay Kit (Thermo Fisher Scientific, Walthman, MA, USA) as per the manufacturer instructions. The MAK311 Peroxide Assay Kit (Sigma-Aldrich, St. Louis, US) was instead used to determine the H_2O_2 content, an assay based on the chromogenic Fe^{+}_{3}-xylenol orange reaction. Briefly, 50 mg GMF- or HMF-exposed samples were grinded in liquid nitrogen and extracted in 1:10 (w/v) mQ ddH_2O. After centrifugation at 15,000 *g* for 10 min, the supernatant was used for the assay according to the manufacturer instructions. A standard H_2O_2 curve was employed for quantification of the H_2O_2 content of samples. Experiments were performed in triplicate.

2.5. Extraction and quantification of plant phytohormones

Approximately 200 mg of leaves, flowers, and fruits from plants grown under GMF or HMF (see section 2.1) were grinded using liquid nitrogen and then extracted with 1 mL of a 1:1 (v/v) mixture of methyl tert-butyl ether (MTBE) and methanol (MetOH). After vortexing, samples were sonicated for 15 min at 4 °C and then 0.5 mL of 0.1 % (v/v) HCl was added. After 5 min, the samples were centrifuged again at 10,000 g for 10 min at 4 °C. The clean MTBE phase was transferred to a new collection tube and dried under nitrogen flow. Finally, the samples were resuspended in 50 μL of a 50 % (v/v) propanol solution. Analytical separation of the different phytohormones was carried out as previously reported (Salem et al., 2020) using an HPLC system (Agilent Technologies system; 1200 HPLC, Agilent Technologies, Santa Clara, CA, USA) equipped with a binary solvent system consisting of water acidified with 0.1 % (v/v) formic acid (solvent A) and methanol acidified with 0.1 % (v/v) formic acid (solvent B). Chromatographic separation was carried on a Kinetex C18 column (130 Å, 1.7 μm, 2.1 × 100 mm) (Phenomenex, Aschaffenburg, Germany). The gradient applied was: 0–8 min 95 % (v/v) solvent A; 8–12 min solvent A was reduced to 75 % (v/v); 12–16 min solvent A was reduced to 55 % (v/v); 16–32 min solvent A was reduced to 25 % (v/v); and then to 5 % (v/v) at 45 min. Solvent A was maintained at this concentration for 10 min. During the chromatographic run, the flow rate was set to 0.2 mL/min, and the injection volume was 20 μL. Before the next injection, the chromatographic conditions were restored to the initial conditions and maintained for 8 min. Phytohormones were detected by a Diode Array Detector (DAD) (Agilent Technologies 1200, Santa Clara, USA) and tandem mass spectrometry (MS/MS) (q-Ion Trap, Bruker Daltonics, HB, Germany), used in multiple reaction monitoring (MRM). For MS/MS analysis, ionization was performed using an electrospray ionization (ESI) source. MRM analysis was used to monitor the different phytohormones and fragmentation pattern, using positive polarity for Indolacetic Acid (IAA), *trans*-Zeatin (tZEA), *trans*-Zeatin riboside (tZEA-rib), gibberellic acids (GA1 and GA4), and isopentenyl adenine, or negative polarity for Abscisic Acid (ABA), ABA-glucoside, salicylic acid (SA) or jasmonic acid (JA). Standard solutions of all phytohormones (Sigma Aldrich, Milan, Italy) were prepared by diluting stock solutions of each hormone in 50 % (v/v) methanol to obtain a range of concentrations from 0.01 to 1000 ng/mL, as previously reported (Salem et al., 2020). Calibration curves were generated by plotting the peak areas of the hormones generated by MS/MS source against their concentrations, while the linear regression was used to quantify phytohormones in the different plant samples. Information related to MW, MS/MS, RT, and λ_{max} are reported in Supplementary Data Set S1. Calibration curves are reported in Supplementary Table S1. The limit of detection (LOD) was calculated based on a signal-to-noise ratio (S/N) greater than 3.3, while the limit of quantification (LOQ) was set at a ratio of S/N greater than 10.

2.6. Extraction and quantification of photosynthetic pigments

The analysis of chlorophylls, chlorophyll degradation products and carotenoids was done according to the protocol of Pumilia and co-workers (2014). Separation and identification of carotenoids, chlorophylls, and chlorophyll degradation products was performed by HPLC-DAD equipped with a C30 column (250 mm 2.1 mm i.d., 3 m, YMC America, Devens, MA, USA) as recently described (Parmagnani et al., 2023). The mobile phases consisted of MetOH,/MTBE/H_2O in 90:3:7 (v/v/v) ratio (Solvent A) and MTBE/MetOH/H_2O in 88:10:2 (v/v/v) ratio (Solvent B). To separate the pigments of interest, solvent A and solvent B were flushed at a constant flow rate of 0.2 mL/min following the ratio described in Parmagnani et al. (2022b). Compounds eluted from the column at different retention times (RT) were detected by DAD set at the following wavelengths: 661 nm (Chl a, Chl a′), 642 nm (Chl b, Chl b′), 667 nm (Pheo 566 a, Pheo a′) and 460 nm (carotenoids). Pigment identification was based on both elution order and UV/Vis spectra examination as previously described (Pumilia et al., 2014). Quantification was performed using pure standards, while pigments without authentic external standards were quantified on calibration curve build on γ-carotene (for *trans*-violaxanthin and *trans*-neoxanthin), chlorophyll *a* (for chlorophyll *a*', pheophytin a and pheophytin a') or chlorophyll *b* (for chlorophyll *b*', pheophytin b and pheophytin b'). Information related to RT, and λ_{max} are reported in Supplementary Data Set S1. Calibration curves are reported in Supplementary Table S1. LOD was calculated based on a S/N greater than 3.3, while LOQ was set at a ratio of S/N greater than 10.

2.7. Extraction and quantification of phenolic compounds

Phenolic compounds were analyzed by the same HPLC-DAD-ESI-MS/MS instrument described in Section 2.5. Chromatographic separation was carried out using a Luna C18 column (150 × 2 mm, 3 µm, Phenomenex, Castel Maggiore, Bologna, Italy) maintained at 40 °C, while the mobile phase consisted of 0.1% (v/v) formic acid in water (Solvent A) and acetonitrile containing 0.1% (v/v) formic acid (Solvent B). Each sample (10 µL) was injected into the system, and the elution from chromatographic system was obtained using with 5% (v/v) Solvent B for the first 4 min, followed by a gradient increase to 100% (v/v) over 45 min. This condition was held for 5 min to complete elution before returning to the starting composition for subsequent analysis. The flow rate was maintained at 200 µL min^{-1} during all the chromatographic analysis. The identification and quantification of compounds for which pure standards were available (quercetin, quercetin-7-glucoside, quercetin-3-rutinoside, kaempferol, catechin, taxifolin, myricetin, naringenin, dihydrokaempferol, and dihydromyricetin) were performed by comparing their UV/Vis spectra, MS/MS patterns, and RT with those of the reference standards. For these compounds, quantification was achieved by constructing calibration curves using MS/MS output and derived from the injection of standard solutions at varying concentrations. All other compounds were putatively identified by comparing their generated mass spectra, UV/Vis profiles, and predicted elution order. Quantification was carried out using the compound that most closely resembled the reference standard. Information related to MW, MS/MS, RT, and λ_{max} are reported in Supplementary Data Set S1. Calibration curves are reported in Supplementary Table S1. For this analysis, LOD was calculated based on a S/N greater than 3.3, while LOQ was set at a ratio of S/N greater than 10.

2.8. Fatty acid profiling

About 10 mg of fresh material from tomato leaves, flowers and fruits were directly esterified with 10% (w/v) boron trifluoride dissolved in methanol in order to obtain fatty acid methyl esters (FAME) as previously described (Cecchin et al., 2022). Briefly, the transesterification reaction was carried out at 80 °C for 1 h in a water bath. Following incubation, the methyl-esterified fatty acids (FAME) were extracted into an organic solvent by adding 500 µL deionized water and 500 µL n-hexane. The addition of the organic solvent was repeated three times to ensure complete recovery of the FAME. Heptadecanoic acid (C17:0) was added before the transesterification reaction and used as the standard to monitor the reaction efficiency. The identification of FAME was performed by injection in GC-MS (5975T, Agilent Technologies, USA) of the sample. Compounds were identified through comparison of mass fragmentation spectra with pure reference standard (for CH_3-C16:0, CH_3-C18:0, and CH_3-C20:0) (Sigma-Aldrich, USA), NIST 98 library and/or by comparison of Kovats indexes. Quantification of each identified FAME was performed using GC-FID (GC-2010 Plus, SHIMADZU, Japan) using analytical standard when available (for CH_3-C16:0, CH_3-C18:0, and CH_3-C20:0). FAMEs for which analytical standards were unavailable were quantified using the most structurally similar compounds, as previously described (Scandiffio et al., 2023). The GC analysis employed helium as the carrier gas, maintained at a constant flow rate of 1 mL/min. Separation was achieved using a ZB5-MS non-polar capillary column (30 m length, 250 µm internal diameter, and 0.25 µm film thickness, consisting of 5% (m/v) phenyl-arylene and 95% (m/v) polydimethylsiloxane) (Phenomenex, USA). The temperature program was as follows: the injector was set to 250 °C; the oven started at 60 °C (held for 1 min), then increased to 180 °C at a rate of 10 °C min^{-1} (held for 1 min), followed by a ramp to 230 °C at 1 °C min^{-1} (held for 2 min), and finally to 320 °C at 15 °C min^{-1} (held for 5 min). The same column and chromatographic conditions were used for both GC-MS and GC-FID analyses. For MS analysis, the ion source was operated at an ionization energy of 70 eV, and data acquisition was performed in the 50–350 m/z range. The quantification was performed in triplicate. Information related to MW, MS/MS and RT are reported in Supplementary Data Set S1. The following abbreviations were used for the identified FAME: C16:0, palmitic acid; C16:1, palmitoleic acid; C16:2, palmitolenic acid; C18:0, stearic acid; C18:1, oleic acid; C18:2, linoleic acid; C18:3, linolenic acid; C20:0, arachidic acid.

2.9. RNA preparation, cDNA cloning and qRT-PCR assays

Total RNA was isolated and purified from three independent biological replicates of tomato leaves, flowers and fruits obtained from different plants (N = 10) by using Peqlab PeqGOLD TriFast reagent (VWR Avantor, Radnor, PA, USA). A BioSpec-nano nanospectrophotometer (Shimadzu, Kyoto, Japan) was used to quantify the extracted RNA. 500 ng of total RNA were used to synthesize cDNA using qScript Ultra Supermix (Quantabio, Beverly, MA, USA), according to the manufacturer's instructions. qRT-PCR assays were performed on a QuantStudio 3 Real-Time PCR System (Applied Biosystems, Foster City, CA) using Perfecta SYBR Green Fastmix (Quantabio, Beverly, MA, USA) with ROX as an internal loading standard. A 15 µL mixture consisting of 7.5 µL 2X Perfecta SYBR Green Fastmix qPCR Master Mix, 0.5 µL cDNA and 250 nM primers (Integrated DNA Technologies, Coralville, IA, US) was used. Controls included non-template controls (water template). PCR conditions were the following for all primers: Hold stage: 2 min at 50 °C, 10 min at 95 °C; PCR stage: 40 cycles of 15 s at 95 °C, 1 min at 60 °C; 10 s at 72 °C; Melting curve stage: 1 min at 60 °C, 1 s at 95 °C. All runs were followed by a melting curve analysis from 55 to 95 °C. All amplification plots were analyzed to obtain Ct values. ACT was used as reference gene. The $\Delta\Delta^{Ct}$ method was used to analyze Ct values. Primers used for real-time PCR were designed using the Primer3 (https://primer3.ut.ee/) software and are reported in Supplementary Table S2.

2.10. Statistical analysis

A Systat 10 software was used for the statistical treatment of data. Data are expressed by mean values and standard deviation. Difference between treatments and controls were assessed by paired *t*-test followed by Bonferroni adjusted probability. Heatmaps were obtained with

Heatmapper (http://www.heatmapper.ca/) (Babicki et al., 2016) by using Pearson clustering with single linkage method. All data are available on Supplementary Data Set S1, whereas all other raw data are available on request.

3. Results

3.1. HMF modulates tomato MagR homologs gene expression

In a recent paper we showed that plants express genes encoding for iron-sulfur cluster assembly (ISCA) homologous to the magnetoreceptor MagR (Parmagnani et al., 2022a). In tomato we found two genes (Iron-sulfur assembly protein IscA-like 1, *Solyc09g009440*, and Iron-sulfur cluster insertion protein erpA 2, *Solyc09g009460*) that are homologous to the magnetosensor *MagR* from *Drosophyla melanogaster* and to two ISCA genes of Arabidopsis (IscA-like 1, At2g16710, and IscA-like 3, At2g36260) (see Supplementary Fig. S1). *Solyc09g009440* was upregulated ($P < 0.05$) by HMF in flowers and ripe fruits, whereas *Solyc09g009460* was strongly upregulated ($P < 0.05$) in the late stages of leaf development (90 DAS), in flowers and ripe fruits and was down-regulated ($P < 0.05$) in unripe fruits (Fig. 1).

3.2. HMF exposure modulates tomato protein content and reduces chlorophyll and chlorophyll precursor/degradation products

Exposure to HMF increased ($P < 0.05$) the protein content in early stages of tomato leaf development (48 and 75 DAS) but had no effect on flowers or unripe/ripe fruits (Fig. 2). The chlorophyll (Chl) content of ripe fruits was almost undetectable (<LOD) and it will not be reported. Tomato exposure to HMF prompted a reduction ($P < 0.05$) of leaf Chl *a* and Chl *b* during early leaf development (48 and 75 DAS), as well as in flowers and unripe fruits; however, no significant effects were found in 90 DAS leaves (Table 1). Under HMF, Chlorophyllide *a'* (Chl *a'*) increased ($P < 0.05$) in early (48 DAS) and late (90 DAS) stages of leaf development as well as in flowers and unripe fruits, whereas the content of Chl *b'* was higher ($P < 0.05$) only in leaves at 90 DAS and in flowers (Table 1). Upon HMF exposure, pheophytin (Pheo) *a* and Pheo *a'* contents were always reduced ($P < 0.05$), whereas the Pheo *b'* content increased ($P < 0.05$) in leaves after 75 and 90 DAS (Table 1).

3.3. HMF affects tomato non-photochemical quenching and electron transfer

Having assessed the significant reduction of Chl *a* and Chl *b*, we evaluated some photosynthetic parameters of photosystem II. Leaves of tomato exposed to HMF showed a decreased ($P < 0.05$) non-photochemical quenching (NPQ), when compared to control plants exposed to GMF mostly at the late stage of development (90 DAS) (Fig. 3B). However, HMF leaves analyzed during flowering time (48 DAS) (Fig. 3A) showed an opposite trend. An increased ($P < 0.05$) photochemical quenching (Qp), or quantum efficiency, and an increased quantum yield (Qy) under actinic light was found during flowering (Supplementary Fig. S2A). In both developmental stages, no significant differences were found in maximal fluorescence (Fm) between HMF and GMF. Moreover, no significant differences were found in 75 DAS leaves (data not shown).

We then assessed the fluorescence kinetics (OJIP analysis) of dark-adapted tomato leaves from plants exposed to either GMF or HMF conditions. In leaves analyzed during flowering (Fig. 3C), exposure to HMF resulted in a significant ($P < 0.05$) increase in fluorescence intensity at all time points, with respect to GMF; whereas no significant differences were found in leaves exposed to HMF during ripe fruit stage (Fig. 3D). S_m (the ratio between the area of the fluorescence induction curve and F_m - F_0) is a measure of the energy required to close all reaction centers (RCs). The more the electrons from the plastoquinone A (QA^-) are transferred into the electron transfer (ET) chain, the longer the fluorescence signals remain below F_m and the bigger S_m becomes. HMF exposed leaves always showed S_m values higher than GMF ($p < 0.05$) (Supplementary Fig. S2B). Moreover, in HMF plants we found a higher ($p < 0.05$) value for N, the turnover number of QA (Supplementary Fig. S2B). N expresses the number of times QA has been reduced in the time span from 0 to t_{Fmax}. In HMF during ripe fruits, a lower flux of dissipated excitation energy at time zero per reaction center (RC), DI_0/RC, was present, with respect to GMF ($p < 0.05$). The DI_0/RC ratio decreases due to the low dissipation of the inactive RCs (Supplementary Fig. S2B).

3.4. HMF modulates tomato carotenoid content and gene expression

Along with chlorophyll, carotenoids play an important role in photosynthesis. The carotenoid content of unripe fruits was

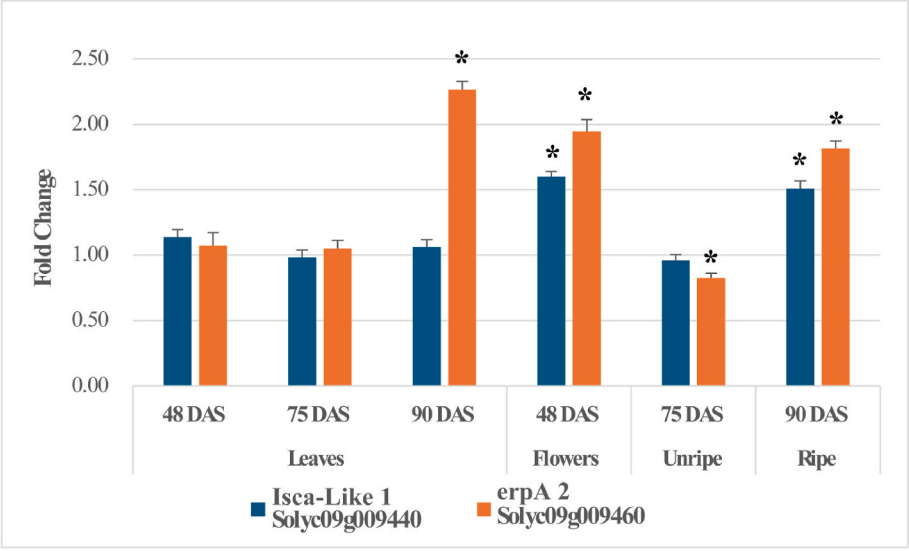

Fig. 1. Fold change expression of the gene coding for ISCA in tomato plants exposed to HMF or GMF. Data are expressed as the HMF/GMF ratio. Metric bars represent standard deviations. Asterisks, where present, indicate statistically significant differences between GMF and HMF conditions, as measured by Tukey's test ($P < 0.05$).

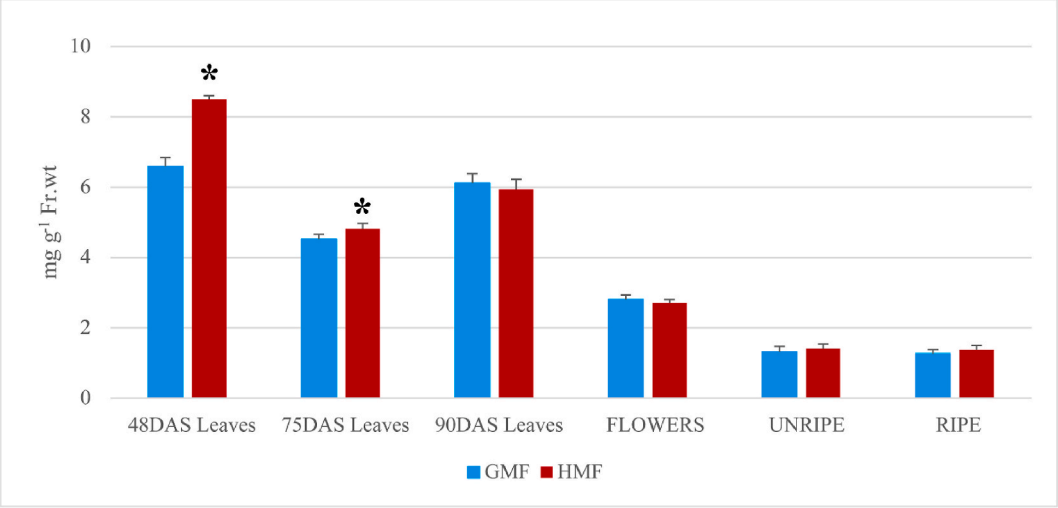

Fig. 2. Protein content of developing leaves (48, 75 and 90 days after sowing, DAS), flowers, unripe and ripe fruits of tomato (*Solanum lycopersicum* cv Microtom) exposed to either hypomagnetic (HMF) or normal (geomagnetic, GMF) conditions. Metric bars indicate standard deviation. Asterisks, where present, indicate statistically significant differences between GMF and HMF conditions, as measured by Tukey's test ($P < 0.05$).

Table 1
Chlorophyll and chlorophyll degradation products of tomato developing leaves, flowers and unripe fruits of plant exposed to HMF and GMF. Mean values are expressed as mg g^{-1} fr.wt (± standard deviation). Asterisk indicated significant ($P < 0.05$) differences between HMF and GMF.

Specification	Leaves						Flowers		Unripe Fruits	
	48 DAS		75 DAS		90 DAS		48 DAS		75 DAS	
	GMF	HMF	GMF	HMF	GMF	HMF	GMF	HMF	GMF	HMF
Chl a	259.56 ± 12.63*	167.87 ± 11.74	332.73 ± 13.62*	213.74 ± 7.32	348.56 ± 13.47*	296.71 ± 7.04	454.31 ± 2.26*	308.1 ± 1.61	5.45 ± 0.17*	2.15 ± 0.07
Chl a'	7.62 ± 0.21*	9.51 ± 0.34	7.32 ± 0.12	7.39 ± 0.18	4.79 ± 0.39*	6.81 ± 0.43	11.83 ± 0.31*	65.02 ± 1.12	0.06 ± 0.01*	0.17 ± 0.01
Chl b	66.05 ± 2.93*	43.48 ± 4.63	82.27 ± 4.42*	51.51 ± 7.44	78.51 ± 4.91	75.55 ± 3.94	65.57 ± 15.24*	53.23 ± 11.01	3.99 ± 0.13*	1.26 ± 0.04
Chl b'	1.91 ± 0.01	1.66 ± 0.01	1.73 ± 0.03*	1.09 ± 0.05	0.21 ± 0.06	0.34 ± 0.07	10.8 ± 0.55*	30.1 ± 3.55	0.19 ± 0.01	0.2 ± 0.01
Chl a/b	3.93 ± 0.21	3.86 ± 0.27	4.04 ± 0.34	4.15 ± 0.37	4.44 ± 0.40	3.93 ± 0.21	6.93 ± 0.42	5.79 ± 0.36	1.37 ± 0.03	1.70 ± 0.05
Pheo a	0.44 ± 0.35	0.24 ± 0.16	7.62 ± 0.31*	3.42 ± 0.09	9.01 ± 0.02*	3.52 ± 0.01	4.05 ± 0.15*	2.37 ± 0.02	0.21 ± 0.01	0.11 ± 0.01
Pheo a'	0.09 ± 4.2	0.03 ± 3.36	96.29 ± 5.65*	48.48 ± 2.27	99.76 ± 0.08*	71.46 ± 4.52	tr	tr	tr	tr
Pheo b	0.59 ± 0.03	tr	2.55 ± 0.11	2.76 ± 0.11	1.3 ± 0.02	1.91 ± 0.03	0.12 ± 0.01	0.14 ± 0.01	tr	tr
Pheo b'	7.63 ± 0.02	tr	21.72 ± 0.72	25.07 ± 1.00	0.42 ± 0.19*	21.05 ± 0.18	0.01 ± 0.001	0.01 ± 0.001	tr	tr

unquantifiable (<LOQ) and is not reported. In ripe fruits, exposure of tomato to HMF prompted a reduction ($P < 0.05$) of the carotenoids 9′-*cis*-α-carotene, 9-*cis*-β-carotene and lycopene as well as the xanthophylls *trans*-neoxanthin and *trans*-violaxanthin. This reduction was accompanied by the increased contents of all other identified carotenoids and of lutein (Table 2). 48 DAS and 75 DAS leaves showed a general reduction ($P < 0.05$) of carotenoids and xanthophylls in HMF exposed plants, whereas an increased ($P < 0.05$) content of γ-carotene and of xanthophylls was found in 90 DAS leaves (Table 2). Flowers of plants exposed to HMF increased ($P < 0.05$) 9′-*cis*-α-carotene, 15-*cis*-β-carotene, all-*trans*-β-carotene and *trans*-neoxanthin, whereas all other identified compounds were reduced ($P < 0.05$) (Table 2).

After observing significant variations in the carotenoid and xanthophyll content of plants exposed to HMF, we analyzed the expression of some genes coding for carotenoid and xanthophyll biosynthetic enzymes. With regards to carotenoids, *PSY2* (*Solyc02g081330*) that codes for a phytoene synthase involved in early carotenoid synthesis (Fraser et al., 2000), was downregulated by HMF in flowers and upregulated in ripe fruits, whereas the expression of *PDS1* (*Solyc03g123760*), that codes for a phytoene desaturase catalyzing the conversion of phytoene to ζ-carotene (Pecker et al., 1992), showed a slight upregulation in 90 DAS leaves and a downregulation in flowers ($P < 0.05$) (Table 3). *ZDS* (*Solyc01g097810*), that codes for a ζ-carotene desaturase (Babu et al., 2020), was upregulated in 48 DAS leaves and ripe fruits, and downregulated in flowers by HMF, whereas *CRTL1* (*Solyc04g040190*), that codes for a lycopene beta-cyclase (Ralley et al., 2016), was upregulated by HMF in 90 DAS leaves ($P < 0.05$) (Table 3). With regards to xanthophylls, in plants under HMF, two cytochromes P450 genes, one encoding a carotenoid β-ring hydroxylase (*CYP97A29*, *Solyc04g051190*) and the other encoding for a carotenoid ε-ring hydroxylase (*CYP97C11*, *Solyc10g083790*) (Stigliani et al., 2011), where both upregulated in 48 DAS leaves and downregulated in flowers ($P < 0.05$). In plants exposed to HMF, *ZEP* (*Solyc02g090890*), encoding a zeaxanthin epoxidase (Burbidge et al., 1997), was downregulated in both 75 DAS leaves and flowers, whereas *VDE* (*Solyc04g050930*), encoding a violaxanthin de-epoxidase (Han et al., 2010), was upregulated in 48 DAS leaves and

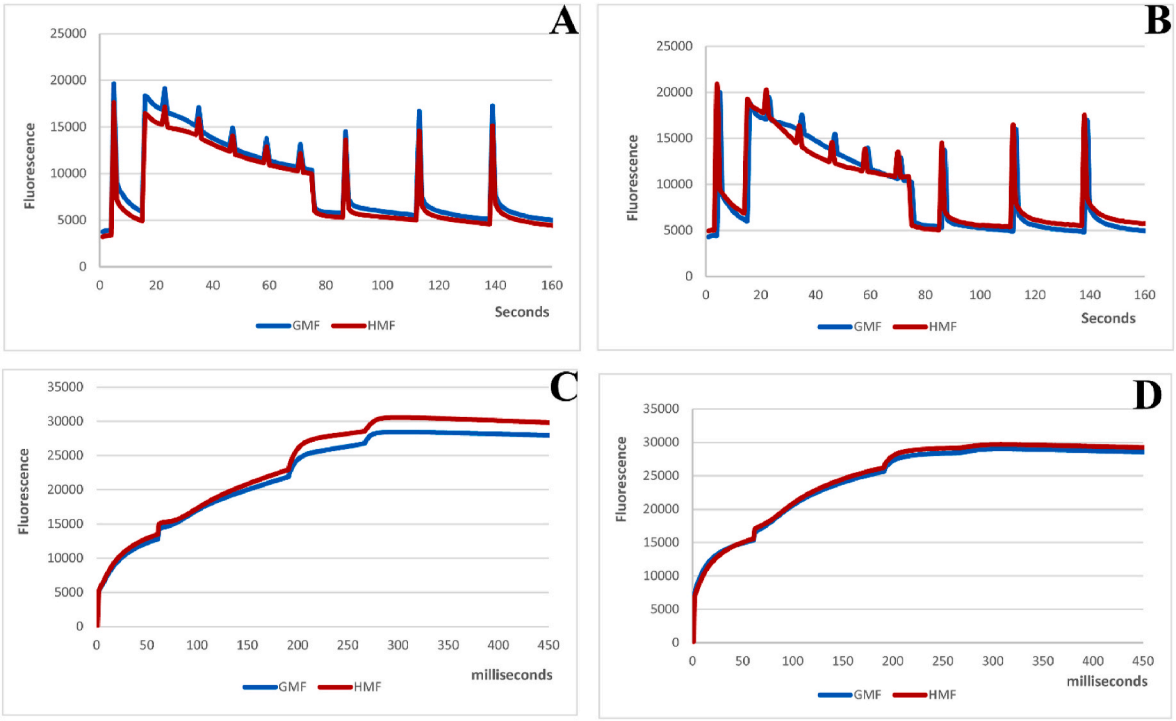

Fig. 3. Chlorophyll fluorescence measurement of Tomato cv Microtom leaves exposed to HMF or GMF. Non-photochemical quenching (NPQ) analysis of plants under either HMF or GMF: A leaves at 48DAS, B leaves at 90DAS. In both **A** and **B**, in the presence of only weak measuring light, the minimal fluorescence (F_0) is seen. Upon a saturating light pulse, the photosynthetic light reactions are saturated and fluorescence reaches the maximum level (Fm). Under actinic light Qp and NPQ lower the fluorescence yield. NPQ is evidenced as the difference between Fm and the measured maximal fluorescence after a saturating light pulse during illumination. OJIP fluorescence transients of dark-adapted tomato leaves plotted on a logarithmic time scale measured on plants exposed to HMF or GMF: **C**, leaves at 48DAS, **D**, leaves at 90DAS.

Table 2
Carotenoid and xanthophyll content of tomato developing leaves, flowers and ripe fruits of plant exposed to HMF and GMF. Mean values are expressed as mg g^{-1} fr.wt (± standard deviation). Asterisk indicated significant differences ($P < 0.05$) between HMF and GMF.

	Leaves						Flowers		Ripe Frutis	
	48 DAS		75 DAS		90 DAS		48 DAS		90 DAS	
	GMF	HMF	GMF	HMF	GMF	HMF	GMF	HMF	GMF	HMF
9′-*cis*-α-carotene	6.89 ± 0.21	6.95 ± 0.29	5.11 ± 0.18*	3.03 ± 0.06	5.94 ± 0.31*	6.47 ± 0.17	0.82 ± 0.03*	1.24 ± 0.04	80.08 ± 3.85*	36.86 ± 1.15
9-*cis*-β-carotene	2.13 ± 0.08*	1.87 ± 0.14	2.35 ± 0.09*	1.27 ± 0.05	2.4 ± 0.12*	2.76 ± 0.05	10.76 ± 0.45*	6.06 ± 0.13	3.52 ± 0.13*	2.51 ± 0.09
all-*trans*-β-carotene	14.32 ± 1.52*	6.66 ± 0.84	33.03 ± 1.05*	17.93 ± 0.76	38.75 ± 0.57	38.14 ± 0.38	3.23 ± 0.10*	4.17 ± 0.12	10.55 ± 0.32*	24.24 ± 0.45
15-*cis*-β-carotene	8.49 ± 0.03*	3.64 ± 0.03	0.59 ± 0.01*	0.28 ± 0.01	0.86 ± 0.33	0.93 ± 0.12	1.43 ± 0.04	1.97 ± 0.09	14.33 ± 0.34*	16.2 ± 0.52
γ-carotene	8.56 ± 0.06*	3.24 ± 0.08	0.34 ± 0.01*	0.13 ± 0.01	1.54 ± 0.24	2.04 ± 0.1	5.71 ± 0.25*	0.99 ± 0.04	4.61 ± 0.13*	6.95 ± 0.41
trans-lutein	11.51 ± 0.66*	8.56 ± 1.32	29.17 ± 0.92	25.28 ± 1.03	33.59 ± 0.41	37.92 ± 0.32	1.27 ± 0.04	1.22 ± 0.04	11.51 ± 0.25*	16.96 ± 0.71
lycopene	tr	tr	tr	tr	8.05 ± 0.42*	5.58 ± 0.24	tr	tr	35.95 ± 1.77*	24.31 ± 1.12
trans-violaxanthin	7.22 ± 0.15	6.89 ± 0.25	3.84 ± 0.11	2.13 ± 0.07	3.18 ± 0.27*	7.15 ± 0.41	15.35 ± 0.36*	6.34 ± 0.28	13.24 ± 0.56*	6.89 ± 0.20
trans-neoxanthin	15.73 ± 0.26*	11.06 ± 0.34	7.04 ± 0.34*	3.57 ± 0.14	6.52 ± 0.59*	8.06 ± 0.32	5.74 ± 0.33*	10.94 ± 0.36	41.22 ± 1.54*	16.86 ± 0.55

tr, traces.

downregulated in flowers (Table 3).

3.5. HMF modulates tomato fatty acid content and gene expression

Tomato leaves exposed to HMF showed increased ($P < 0.05$) contents of C16:0, C16:1, C16:2, C18:2 and C18:3 in 48 DAS leaves (Table 4). C18:0 was increased ($P < 0.05$) by HMF only in 90 DAS leaves. In flowers, HMF exposure reduced ($P < 0.05$) the content of C16:0, C18:2, C18:3 and C20:0, whereas in unripe fruits the content of the same FAs was increased ($P < 0.05$). In ripe fruits, HMF prompted a reduction ($P < 0.05$) of both C18:3 and C20:0 (Table 4).

The expression of some genes involved in FAs metabolism was then assessed. *ACP* (*Solyc00g041190*), coding for the acyl carrier protein involved in FA synthesis (Zhou et al., 2022), was upregulated by HMF in late stages of leaf development (90 DAS) and in flowers and unripe and ripe fruits (Table 5). Four FA desaturases were modulated by HMF; in

Table 3
Fold change expression of gene coding for carotenoid biosynthesis in tomato plants exposed to HMF and GMF. Data are expressed as the HMF/GMF ratio (± standard deviation). Asterisk indicates significant ($P < 0.05$) differences between HMF and GMF.

Gene	Leaves			Flowers	Unripe fruits	Ripe fruits
	48 DAS	75 DAS	90 DAS	48 DAS	75 DAS	90 DAS
PSY2	1.09 ± 0.06	0.72 ± 0.06	0.79 ± 0.03	0.64* ± 0.04	0.81 ± 0.04	1.39* ± 0.02
PDS1	1.11 ± 0.05	0.88 ± 0.03	1.17* ± 0.02	0.66* ± 0.02	0.71 ± 0.02	1.24 ± 0.02
ZDS	1.20* ± 0.02	0.88 ± 0.01	1.11 ± 0.02	0.72* ± 0.01	1.56* ± 0.12	1.64* ± 0.08
CRTL1	0.94 ± 0.12	0.88 ± 0.04	1.28* ± 0.11	0.92 ± 0.03	1.47* ± 0.13	1.23 ± 0.05
CYP97A29	1.23* ± 0.03	0.90 ± 0.03	0.91 ± 0.019	0.71* ± 0.02	1.57* ± 0.10	1.04 ± 0.09
CYP97C11	1.12* ± 0.03	0.87 ± 0.01	1.06 ± 0.04	0.85* ± 0.03	2.18* ± 0.10	1.20 ± 0.07
ZEP	1.21 ± 0.04	0.79* ± 0.05	0.99 ± 0.03	0.64* ± 0.03	1.11 ± 0.08	1.00 ± 0.05
VDE	1.16* ± 0.02	0.85 ± 0.02	1.00 ± 0.05	0.65* ± 0.02	2.32* ± 0.19	1.06 ± 0.15

Table 4
Fatty acid composition of tomato developing leaves, flowers and fruits exposed to GMF and HMF. Data are expressed as μg g^{-1} fr. wt. (± standard deviation), asterisk indicates significant ($P < 0.05$) differences between HMF and GMF.

Organ	Condition	Fatty acids							
		C16:0	C16:1	C16:2	C18:0	C18:1	C18:2	C18:3	C20:0
Leaves 48 DAS	GMF	982.85 ±85.14	271.97 ±31.11	348.24 ±35.86	223.76 ±20.96	205.49 ±19.66	484.51 ±76.75	889.33 ±122.86	184.25 ±19.45
	HMF	1483.46* ±107.65	415.28* ±68.23	560.99* ±64.98	283.19 ±64.14	254.77 ±62.3	909.36* ±70.13	1943.38* ±121.42	218.22 ±60.82
Leaves 75 DAS	GMF	1250.05 ±224.09	299.06 ±67.47	286.05 ±58.72	291.91 ±65.43	238.1 ±58.13	527.27 ±99.6	996.45 ±163.03	227.82 ±56.23
	HMF	1153.97 ±127.1	258.42 ±36.88	243.57 ±32.86	267.64 ±38.14	210.05 ±32.83	539.21 ±49.17	900.23 ±60.05	215.13 ±32.49
Leaves 90 DAS	GMF	1072.24 ±160.67	221.13 ±26.92	199.51 ±24.12	230.38 ±28.73	169.54 ±19.44	465.88 ±72.7	949.35 ±158.08	202.59 ±27.21
	HMF	1164.61 ±0.98	296.21 ±20.52	259.16 ±23.41	314.37* ±20.24	243.27 ±22.86	531.75 ±23.51	989.86 ±15.43	302.59 ±19.42
Flowers 48 DAS	GMF	1017.96 ±4.78	tr	tr	254.44 ±11.48	tr	871.68 ±62.91	966.44 ±23.21	63.21 ±3.3
	HMF	772.65* ±16.72	tr	tr	174.36 ±28.56	tr	586.90* ±83.85	597.46* ±128.76	43.33* ±5.93
Unripe Fruit 75 DAS	GMF	78.22 ±3.27	tr	tr	11.03 ±1.3	tr	120.32 ±6.68	76.84 ±2.41	1.68 ±0.37
	HMF	118.73* ±7.34	tr	tr	17.38 ±1.23	tr	218.50* ±22.35	117.57* ±15.01	2.89* ±0.60
Ripe Fruit 90 DAS	GMF	89.33 ±10.74	tr	tr	18.35 ±8.63	tr	65.42 ±11	116.17 ±18.66	1.06 ±0.56
	HMF	70.47 ±6.49	tr	tr	9.39 ±1.43	tr	59.48 ±5.01	27.23* ±3.19	0.52* ±0.10

tr, traces.

Table 5
Fold change expression of gene coding for fatty acid metabolism in tomato plants exposed to HMF and GMF. Data are expressed as the HMF/GMF ratio (± standard deviation). Asterisk indicates significant ($P < 0.05$) differences between HMF and GMF.

Gene	Leaves 48 DAS	Leaves 75 DAS	Leaves 90 DAS	Flowers	Unripe fruits	Ripe fruits
ACP	0.82 ± 0.16	0.82 ± 0.10	3.80* ± 0.28	1.55* ± 0.30	1.26* ± 0.28	1.52* ± 0.34
SAD	1.05 ± 0.05	1.07 ± 0.02	0.50* ± 0.04	1.40* ± 0.07	2.10* ± 0.05	0.88 ± 0.03
Fatty Acid Desaturase	1.16 ± 0.09	1.94* ± 0.51	32.10* ± 4.79	2.67* ± 0.21	2.97* ± 0.54	0.83 ± 0.22
FAD	1.24 ± 0.07	0.56* ± 0.01	0.21* ± 0.03	1.42* ± 0.08	4.40* ± 0.09	1.02 ± 0.05
FAD2	1.12 ± 0.10	0.93 ± 0.20	13.50* ± 1.04	1.54* ± 0.14	0.95 ± 0.11	1.02 ± 0.04

particular, *SAD* (*Solyc03g063110*) coding for a stearoyl-acyl carrier protein desaturase, was downregulated in 90 DAS leaves, but was upregulated in flowers and in unripe fruits, whereas a FA desaturase (*Solyc12g100230*) coding for an enzyme that catalyzes the introduction of an omega-3 double bond into the FA hydrocarbon chain was upregulated in 75 DAS leaves, in flowers and in unripe fruits and strongly upregulated in 90 DAS leaves (Table 5). A gene coding for an omega-3 fatty acid desaturase (*FAD*, *Solyc06g051400*) belonging to tomato immune-related genes, was downregulated in 75 and 90 DAS leaves and upregulated in flowers and unripe fruits; whereas a gene coding for an omega-6 FA desaturase (*FAD2*, *Solyc01g006430*) was upregulated in flowers and strongly upregulated in 90 DAS leaves (Nakamura et al., 2016) (Table 5).

3.6. HMF modulates ROS production levels and gene expression

Exposure of tomato plants to HMF decreased ($P < 0.05$) the production of H_2O_2 in both 48 and 75 DAS leaves and in flowers; however, the H_2O_2 content, although much lower compared to leaves, increased ($P < 0.05$) in both unripe and ripe fruits (Fig. 4).

We then analyzed the expression of genes coding for some ROS producing and scavenging enzymes (Table 6). The expression of *RBOH1* (*Solyc08g081690*), that codes for the respiratory burst homolog that generates the superoxide anion (Xu et al., 2021), was downregulated in

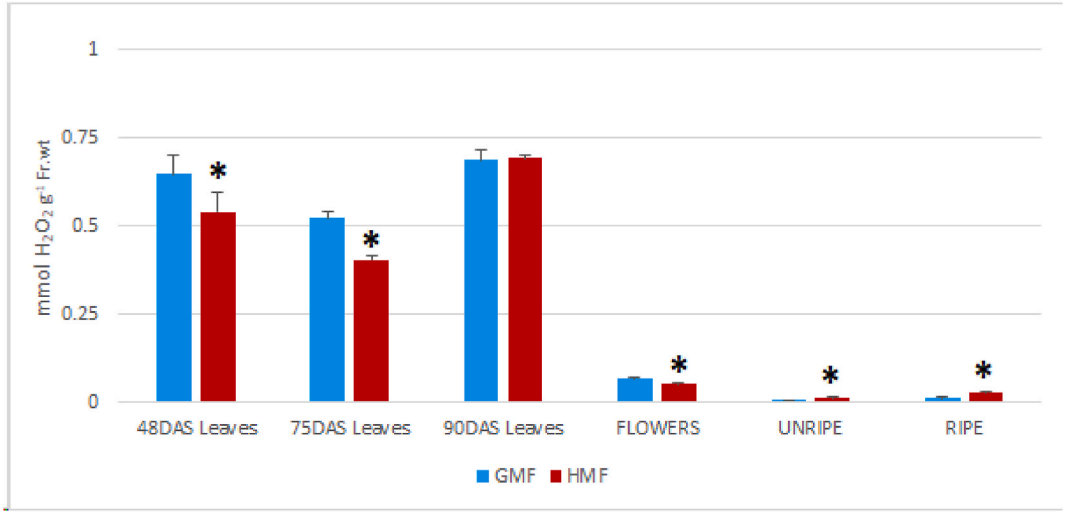

Fig. 4. H_2O_2 production in tomato developing leaves, flowers, unripe and ripe fruits of plant exposed to HMF and GMF. Metric bars indicate standard deviation. Asterisks, where present, indicate statistically significant differences between GMF and HMF conditions, as measured by Tukey's test ($P < 0.05$).

Table 6
Fold change expression of genes coding for ROS production and scavenging in tomato plants exposed to HMF and GMF. Data are expressed as the HMF/GMF ratio (± standard deviation). Asterisk indicates significant ($P < 0.05$) differences between HMF and GMF.

Gene	Leaves			Flowers	Unripe fruits	Ripe fruits
	48 DAS	75 DAS	90 DAS	48 DAS	75 DAS	90 DAS
RBOH	1.11 ± 0.02	0.96 ± 0.04	0.71* ± 0.01	0.64* ± 0.03	7.19* ± 0.21	0.96 ± 0.04
SOD	1.20* ± 0.05	1.05 ± 0.04	1.23* ± 0.23	1.35* ± 0.20	1.21 ± 0.01	1.70* ± 0.01
CAT	1.04 ± 0.04	0.91* ± 0.03	1.07 ± 0.02	1.12 ± 0.09	0.9 ± 0.02	1.02 ± 0.03
APX	1.05 ± 0.01	0.82* ± 0.01	1.46* ± 0.02	1.89* ± 0.10	1.65* ± 0.07	1.39* ± 0.01
GPXLE1	1.16 ± 0.02	0.94 ± 0.01	1.09 ± 0.02	1.71* ± 0.21	1.61* ± 0.08	1.94* ± 0.41
GPXLE2	1.29* ± 0.01	0.97 ± 0.03	1.46* ± 0.05	1.33* ± 0.08	0.97 ± 0.03	1.70* ± 0.20
GSR	1.10 ± 0.02	0.93 ± 0.02	1.00 ± 0.01	0.80* ± 0.01	1.11 ± 0.01	1.26* ± 0.08
GR	1.09 ± 0.01	1.00 ± 0.01	0.98 ± 0.04	0.71* ± 0.3	0.72 ± 0.01	1.27* ± 0.03

90 DAS leaves and flowers and upregulated in unripe fruits by HMF, whereas *SODCC1* (*Solyc01g067740*), coding for a Cu-Zn superoxide dismutase that produces H_2O_2 (Perltreves and Galun, 1991), showed an opposite trend, being upregulated by HMF in 48 and 90 DAS leaves, in flowers and in ripe fruits (Table 4). The next genes are coding for enzymes that remove H_2O_2. In 75 DAS leaves, HMF slightly downregulated catalase (*CAT1*, *Solyc12g094620*) (Soydam Aydin et al., 2016), while cytosolic ascorbate peroxidase 1 (*APX1*, *Solyc06g005160*) (Zou et al., 2005) was also downregulated in 75 DAS leaves but showed an upregulation in 90 DAS leaves, flowers and in both unripe and ripe fruits (Table 6). Two glutathione peroxidase-like encoding genes, *GPXLE1* (*Solyc08g080940*) and *GPXLE2* (*Solyc12g056230*) (Depège et al., 1998), showed differential expression upon HMF: *GPXLE1* was upregulated in flowers and in both unripe and ripe fruits, whereas *GPXLE2* was upregulated in 48 and 90 DAS leaves, flowers and ripe fruits, but lacked the upregulation in unripe fruits (Table 6). Under HMF, *GSR* (*Solyc09g091840*) coding for a glutathione-disulfide reductase that catalyzes the reduction of glutathione disulfide to the sulfhydryl form glutathione (Jegadeesan et al., 2018), and glutathione reductase (*GR*, *Solyc09g065900*), coding for glutathione reductase catalyzing the reduction of the oxidized glutathione disulphide form (GSSG) to the reduced one (GSH) (Noctor and Foyer, 1998), were downregulated in flowers and upregulated in ripe fruits (Table 6).

3.7. HMF modulates tomato phenolic compounds content and gene expression

HPLC-DAD-MS/MS analyses of developing leaves, flowers and fruits extracts from tomato plants exposed to either GMF or HMF allowed the characterization of 90 polyphenols, including aglycone and glycosylated forms of apigenin, catechin, dihydrokaempferol, kaempferol, dihydromyricetin, myricetin, naringenin, quercetin, rhamnetin and taxifolin. In general, exposure to HMF increased the content of apigenin, catechin, dihydrokaempferol and dihydromyricetin (aglycones and glycosides) and reduced the amount of quercetin, rhamnetin and taxifolin (aglycones and glycosides) (See Supplementary Data Set S1).

To identify which flavonoids were modulated in tomato organs, we calculated the HMF/GMF ratio and considered those molecules that were modulated with a fold change higher than 1.5 or lower than 0.67. Another inclusion criterium in our elaboration was the presence of the same compound in at least two organs. Fig. 4 shows the heatmap generated by this elaboration (see also raw data in Supplementary Data Set S1). Four main flavonoid structures (three flavonols, taxifolin, catechin and rhamnetin; and a flavone, apigenin), were differentially modulated by HMF. In general, polyphenols of flowers show a low statistical relation (high Pearsonian distances) with those of the other organs, whereas a close statistical relation (low Pearsonian distances) is present between unripe and ripe fruits and among the developing leaves. Most of the flavonoids reduced by HMF in fruits showed an opposite trend in leaves. For instance, apigenin (sambubioside, rhamnoside and glucuronide) and taxifolin (glucoside, diglucoside, rutinoside and arabinoside), increased in flowers and decreased at all leaf stages of development, whereas the flower content of catechin (sambubioside, diglucoside, rhamnoside, arabinoside and rutinoside) was reduced as in most of leaves (Fig. 5). In response to HMF, an opposite trend was found between unripe and ripe fruits for catechin glucuronide and taxifolin (glucoside, rutinoside and arabinoside), whereas 48 DAS leaves showed a general reduction of most of the selected flavonoids, including all

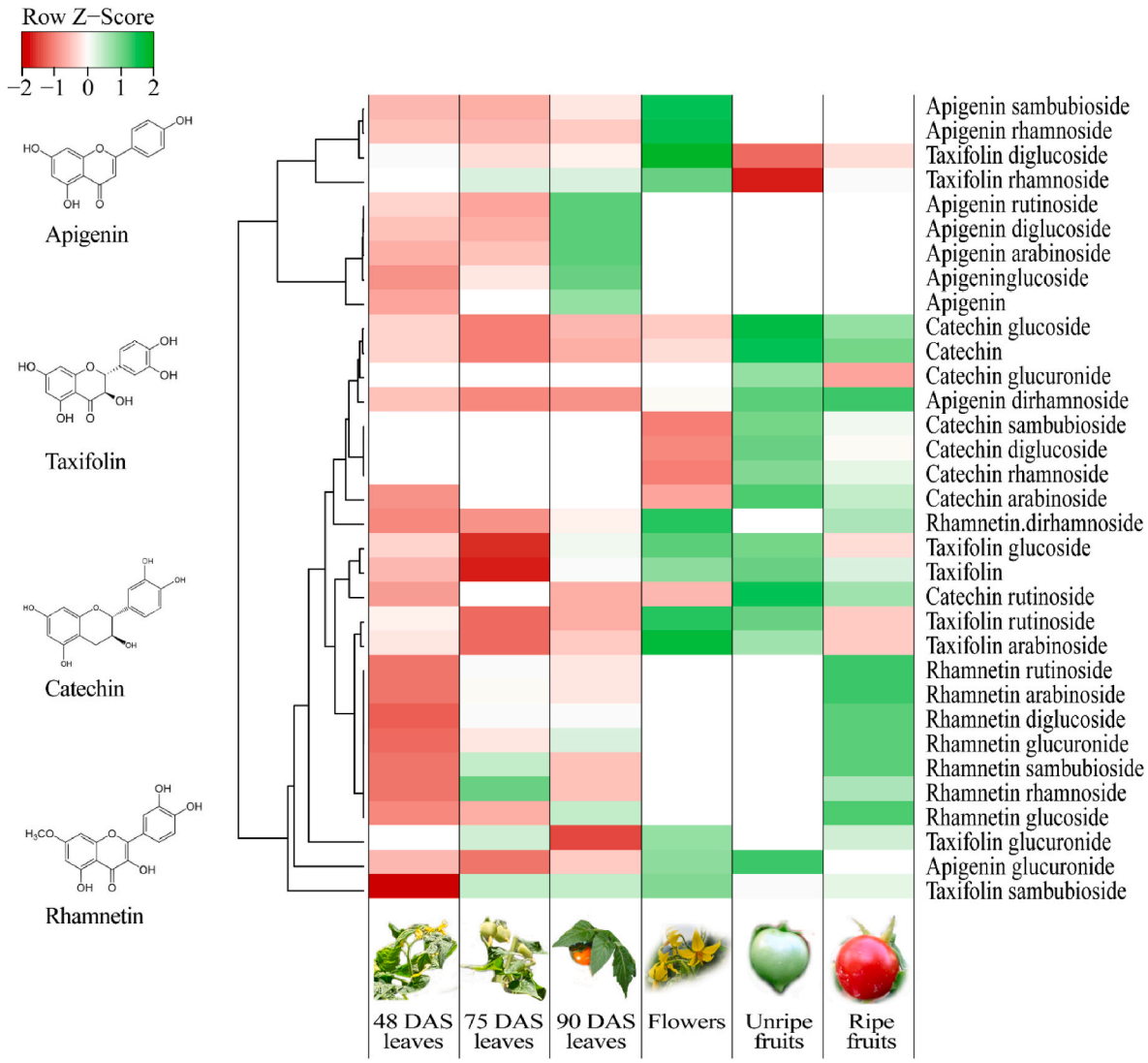

Fig. 5. Heatmap generated by considering the HMF/GMF ratio of tomato polyphenols modulated in at least two organs possessing a fold change ration (HMF/GMF) > 1.5 or < 0.67. Clustering was obtained with Pearsonian single linkage method. Polyphenols of flowers show a low statistical relation (high Pearsonian distances) with those of the other organs, whereas a close statistical relation (low Pearsonian distances) is present between unripe and ripe fruits and among the developing leaves.

rhamnetin glycosides and taxifolin sambubioside. The latter increased in the other leaf development, whereas an opposite trend for apigenin (rutinoside, glucoside, diglucoside and arabinoside) was found in 90 DAS leaves, with respect to the other two leaf developmental stages (Fig. 5).

Upon analysing of all other compounds, we observed that HMF exposure predominantly modulated apigenin, kaempferol arabinoside, and naringenin rhamnoside in the leaves. In contrast, apigenin glucuronide, apigenin dirhamnoside, quercetin, and myricetin glucoside were exclusively modulated in unripe fruits, whereas apigenin glucuronide and dirhamnoside were only affected in ripe fruits (see also Supplementary Data Set S1).

The expression of some genes coding for polyphenol metabolism was then assessed. A gene coding for chalcone synthase 1 (*CHS1*, *Solyc09g091510*), involved in the early steps of flavonoids biosynthesis (Oneill et al., 1990), was upregulated by HMF in 48 and 90 DAS leaves as well as in flowers and unripe fruits (Table 7). Chalcone synthase 2 (*CHS2*, *Solyc05g053550*) showed almost the same pattern, but with a stronger upregulation in 48 DAS leaves and no effects were observed in unripe fruits (Table 7). The next step in flavonoid metabolism is

Table 7
Fold change expression of genes coding for polyphenols from plants exposed to HMF and GMF. Data are expressed as the HMF/GMF ratio (± standard deviation). Asterisk indicates significant (P < 0.05) differences between HMF and GMF.

Gene	Leaves 48 DAS	Leaves 75 DAS	Leaves 90 DAS	Flowers	Unripe fruits	Ripe fruits
CHS1	1.85* ± 0.09	0.92 ± 0.05	2.18* ± 0.09	1.65* ± 0.09	6.68* ± 0.64	0.85 ± 0.07
CHS2	7.17* ± 0.46	1.56* ± 0.12	2.78* ± 0.09	1.21* ± 0.03	0.99 ± 0.03	0.96 ± 0.04
Solyc05g010310 (CHI)	0.96 ± 0.07	2.03* ± 0.22	2.47* ± 0.26	2.67* ± 0.06	1.53* ± 0.18	1.53* ± 0.13
Solyc05g010320 (CHI)	1.80* ± 0.10	1.15 ± 0.07	1.29 ± 0.07	1.05 ± 0.03	3.79* ± 0.10	1.07 ± 0.13
F3HA	1.29 ± 0.35	0.63* ± 0.02	0.68* ± 0.12	3.01* ± 0.09	56.60* ± 5.47	1.76* ± 0.45
F3HB	1.52* ± 0.11	1.72* ± 0.14	1.53* ± 0.13	2.17* ± 0.08	0.66* ± 0.02	1.24 ± 0.03

catalyzed by chalcone isomerase (CHI) (Kawasaki et al., 2014). A gene coding for a *CHI* isoform (*Solyc05g010310*) was always upregulated by HMF (with the sole exception for 48 DAS leaves), whereas a gene coding for another CHI isoform (*Solyc05g010320*) was only upregulated in 48 DAS leaves and in unripe fruits (Table 7). The transition of flavanones to dihydroflavonols is catalyzed by flavanone 3-hydroxylase (*F3HA*, *Solyc06g073080*) (Meng et al., 2015) that under our experimental conditions was downregulated in 75 and 90 DAS leaves, upregulated in flowers and ripe fruits, and strongly upregulated in unripe fruits by exposure to HMF; whereas another isoform of flavanone 3-hydroxylase (*F3HB*, *Solyc02g083860*) showed an opposite trend (Table 7).

3.8. HMF modulates tomato phytohormone content and gene expression

Exposure of tomato to HMF caused the modulation of several phytohormones, among which the growth promoting phytohormones were differentially modulated (Table 8). Upon exposure to HMF, indoleacetic acid (IAA) was reduced in 75 DAS leaves but was increased in 90 DAS leaves, flowers and unripe fruits, whereas gibberellic acid 1 (GA_1) was mostly reduced in leaves at all stages of development and in ripe fruits and was increased in unripe fruits (Table 8). GA_4 was reduced also in 48 DAS leaves and flowers but showed an opposite trend with respect to GA1 in 90 DAS leaves and ripe fruits (Table 8). *Trans*-zeatin did not show significant changes in all sampled organs; however, upon exposure to HMF, zeatin riboside was always reduced, whereas iP was reduced in 48 DAS leaves and in unripe fruits and was increased in 90 DAS leaves and flowers (Table 8).

With regards to growth inhibitory and stress responsive phytohormones, exposure to HMF reduced abscisic acid (ABA) content of 75 DAS and 90 DAS leaves and unripe fruits, whereas the sugar bound ABA-glucose ester (ABA-GE) was increased by HMF in all organs under study (Table 8). HMF prompted a slight increase of salicylic acid only in 90 DAS leaves, whereas jasmonic acid (JA) was decreased in leaves at all developmental stages (Table 8).

When genes coding for phytohormone transport and signaling were assayed we found modulation of several genes (Table 9). With regards to auxins, upon HMF a gene coding for a small auxin up-regulated RNA (*SlSAUR1*, *Solyc01g091030*) (Wu et al., 2012) was downregulated in 75 DAS and 90 DAS leaves, unripe and ripe fruits, but was upregulated in flowers. The auxin efflux facilitators involved in polar auxin transport *PIN1* (*Solyc03g118740*), implicated in regulating the polar auxin transport (Kharshiing et al., 2010), was upregulated by HMF in 48 DAS and 90 DAS leaves, flowers and particularly in unripe fruits. On the other hand, *PIN2* (*Solyc07g006900*) that is also involved in gravitropism (Teale et al., 2008), was upregulated during leaf development and in unripe fruits, but was downregulated in ripe fruits. *PIN3* (*Solyc04g007690*), that codes for a protein that is involved in the asymmetric auxin accumulation by determining the direction of auxin flux (Friml et al., 2002), was downregulated in 75 DAS and 90 DAS leaves and strongly upregulated in unripe fruits (Table 9).

The gene expression of *gibberellin 20-oxidase 1* (*GA20ox1*, *Solyc03g006880*) was strongly upregulated by HMF in unripe fruits and was downregulated in 75 DAS and 90 DAS leaves and in flowers. *Gibberellin 2-oxidase 1* (*GA2ox1*, *Solyc05g053340*), that codes for an enzyme involved in GA_4 transformation to GA_{34} (Schrager-Lavelle et al., 2019), was downregulated in 48 DAS and 75 DAS leaves and in ripe fruits and strongly upregulated in unripe fruits and to a lower extent in 90 DAS leaves and flowers, whereas *gibberellin 2-oxidase 2* (*GA2ox2*, *Solyc03g116290*) showed a similar trend for 90 DAS leaves and unripe fruits and an opposite trend for 75 DAS leaves, flowers and ripe fruits (Table 9).

The gene *LOG* (*Solyc09g007830*), that codes for a cytokinin riboside 5′-monophosphate phosphoribohydrolase, was downregulated in 90 DAS leaves and ripe fruits and strongly upregulated in unripe fruits. The gene coding for cytokinin oxidase 2 (*SlCKX2*, *Solyc01g088160*) was downregulated in 75 DAS and 90 DAS leaves and upregulated in flowers and unripe fruits. The cytokinin response factor *CRF2* (*Solyc08g081960*), which belongs to AP2/ERF transcription factors induced by cytokinin (Shi et al., 2012), was downregulated only in 75 DAS and 90 DAS leaves, whereas all other organs showed an increased gene expression. The type-A response regulator 2 (*RRA2*, *Solyc02g071220*), is also involved in response to cytokinin (Matsuo et al., 2012). *RRA2* was downregulated in flowers and upregulated in all other organs (Table 9).

Aldehyde oxidase 1 (*AO1*, *Solyc11g071620*) was downregulated in 75 DAS and 90 DAS leaves. The gene coding for the *PYL6* (*Solyc03g095780*) was downregulated in 90 DAS leaves and strongly upregulated in unripe fruits. This gene was undetectable in ripe fruits under HMF (Table 9). *AIM1* was strongly upregulated in 90 DAS leaves and in flowers and strongly downregulated in fruits. The ABA stress ripening gene *ASR1* (*Solyc04g071610*) was almost always upregulated by HMF,

Table 8
Quantitative determination of tomato developing leaves, flowers and fruits phytohormone content in plants exposed to either GMF or HMF. Data are expressed as mean value ± standard deviation from three different replicates. Asterisk indicated significant differences between HMF and GMF.

Hormones	Leaves						Flowers		Unripe Fruits		Ripe Fruits	
	48 DAS		75 DAS		90 DAS		48 DAS		75 DAS		90 DAS	
	GMF	HMF	GMF	HMF	GMF	HMF	GMF	HMF	GMF	HMF	GMF	HMF
IAA (μg g^{-1} FW)	12.61 ±0.60	12.90 ±0.34	11.27 ±0.27	8.47* ±0.40	14.52 ±0.58	16.35* ±0.96	6.64 ±0.22	7.65* ±0.38	2.81 ±0.1	3.17* ±0.1	2.56 ±0.12	2.63 ±0.1
GA_1 (ng g^{-1} FW)	34.07 ±0.59	31.84 ±0.97	13.33 ±0.68	10.15* ±0.31	17.93 ±0.49	15.10* ±0.5	5.51 ±0.18	5.85 ±0.20	2.20 ±0.06	3.75* ±0.09	37.77 ±1.55	19.39* ±0.41
GA_4 (ng g^{-1} FW)	15.17 ±0.54	7.42* ±0.36	32.17 ±1.77	23.51* ±0.87	44.51 ±2.21	74.96* ±2.65	106.74 ±4.11	40.22* ±1.76	7.52 ±0.35	35.2* ±1.32	2.47 ±0.09	37.47* ±1.42
iP (ng g^{-1} FW)	226.00 ±10.51	160.91* ±5.88	186.19 ±9.07	199.16 ±4.56	359.59 ±11.39	452.63* ±18.78	19.87 ±1.08	34.82* ±0.81	24.75 ±0.66	14.54* ±0.52	16.99 ±0.82	19.33 ±0.53
zeatin riboside (μg g^{-1} FW)	7.49 ±0.32	tr	9.42 ±0.22	tr	11.33 ±0.36	tr	4.01 ±0.13	tr	0.48 ±0.03	tr	0.68 ±0.02	tr
trans-zeatin (μg g^{-1} FW)	53.23 ±2.91	49.56 ±2.32	45.94 ±1.99	48.05 ±2.71	59.16 ±2.56	60.27 ±1.54	11.15 ±0.52	11.46 ±0.31	3.84 ±0.14	4.76 ±0.18	4.01 ±0.16	4.17 ±0.17
ABA (μg g^{-1} FW)	15.07 ±0.37	14.32 ±0.59	16.67 ±0.33	13.30* ±0.7	30.00 ±1.14	18.55* ±0.42	40.75 ±1.3	46.2 ±1.98	5.83 ±0.32	3.29* ±0.11	2.70 ±0.11	2.22 ±0.08
ABA-GE (μg g^{-1} FW)	28.31 ±1.03	97.02* ±2.77	31.7 ±1.76	63.48* ±1.84	13.72 ±0.59	37.41* ±1.42	15.59 ±0.57	31.32* ±1.08	4.52 ±0.14	11.32* ±0.40	3.21 ±0.13	6.36* ±0.23
SA (μg g^{-1} FW)	6.22 ±0.20	7.45 ±0.36	10.87 ±0.46	12.54 ±0.23	4.69 ±0.18	7.71* ±0.24	1.94 ±0.07	2.23 ±0.06	0.50 ±0.02	0.48 ±0.03	0.49 ±0.02	0.43 ±0.02
JA (μg g^{-1} FW)	154.3 ±8.12	129.18* ±5.11	66.55 ±3.56	45.70* ±2.04	72.88 ±3.07	60.55* ±1.86	3.23 ±0.11	3.07 ±0.11	1.65 ±0.09	1.94 ±0.09	1.57 ±0.04	1.65 ±0.06

tr, traces.

Table 9
Fold change expression of genes coding for phytohormones in tomato plants exposed to HMF and GMF. Data are expressed as the HMF/GMF ratio (± standard deviation). Asterisk indicates significant ($P < 0.05$) differences between HMF and GMF.

Hormone	Gene	Leaves 48 DAS	Leaves 75 DAS	Leaves 90 DAS	Flowers	Unripe fruits	Ripe fruits
Auxin	*SlSAUR1*	1.01 ± 0.02	0.71* ± 0.01	0.53* ± 0.02	5.68* ± 0.44	0.42* ± 0.02	0.59* ± 0.05
	PIN1	1.25* ± 0.11	1.03 ± 0.05	1.86* ± 0.14	1.24* ± 0.03	6.42* ± 0.44	0.96 ± 0.26
	PIN2	1.57* ± 0.11	1.87* ± 0.21	1.56* ± 0.22	0.89 ± 0.12	4.42* ± 0.86	0.74* ± 0.04
	PIN3	1.09 ± 0.09	0.64* ± 0.03	0.66* ± 0.11	0.97 ± 0.02	67.98* ± 12.4	nd
Gibberellin	*GA20OX1*	1.12 ± 0.07	0.31* ± 0.02	0.61* ± 0.03	0.78 ± 0.02	240.33* ± 25.7	0.93 ± 0.11
	GA2OX1	0.73* ± 0.11	0.73* ± 0.08	2.89* ± 0.45	3.24* ± 0.25	10.87* ± 0.63	0.46* ± 0.03
	GA2OX2	1.51 ± 0.32	1.56* ± 0.13	8.12* ± 0.65	0.93 ± 0.26	6.28* ± 2.29	2.99* ± 0.13
Cytokinin	*LOG*	1.12 ± 0.02	1.04 ± 0.06	0.75* ± 0.05	0.88 ± 0.11	21.49* ± 0.72	0.65* ± 0.15
	SlCKX2	1.16 ± 0.09	0.55* ± 0.02	0.41* ± 0.06	3.73* ± 0.34	40.19* ± 2.34	nd
	CRF2	2.20* ± 0.28	0.68* ± 0.11	0.79* ± 0.07	1.72* ± 0.21	8.31* ± 0.41	1.55 ± 0.06
	RRA2	2.24* ± 0.14	1.37* ± 0.05	2.22* ± 0.08	0.64* ± 0.11	2.28* ± 0.21	1.64* ± 0.25
ABA	*AO1*	1.07 ± 0.04	0.62* ± 0.07	0.68* ± 0.11	0.88 ± 0.05	0.79 ± 0.06	0.87 ± 0.13
	PYL6	1.14 ± 0.21	1.14 ± 0.27	0.61* ± 0.13	1.79* ± 0.21	50.68* ± 9.33	nd in HMF
	AIM1	0.87 ± 0.05	0.89 ± 0.26	14.06* ± 2.03	6.08* ± 2.22	0.26* ± 0.04	0.31* ± 0.05
	ASR1	1.90* ± 0.04	1.01 ± 0.05	1.78* ± 0.08	1.97* ± 0.09	0.37* ± 0.05	1.31* ± 0.09
Jasmonate	*COI1*	1.17* ± 0.04	0.86 ± 0.09	1.16* ± 0.02	1.18* ± 0.03	0.84 ± 0.09	1.07 ± 0.03
	JAZ1	1.35 ± 0.09	0.96 ± 0.03	0.78 ± 0.03	4.29* ± 0.15	4.47* ± 0.35	2.10* ± 0.45
Salicylate	*SAMT*	1.44* ± 0.18	0.89 ± 0.09	2.57* ± 0.92	1.84* ± 0.07	5.36* ± 0.82	0.64* ± 0.11
	Solyc02g077530	0.71 ± 0.16	1.36 ± 0.32	32.97* ± 10.24	0.90 ± 0.07	1.56 ± 0.15	0.85 ± 0.14

except for 75 DAS leaves and in unripe fruits, where the gene was downregulated (Table 9).

The coronatine-insensitive 1 gene (*COI1*, *Solyc05g052620*) was slightly upregulated by HMF in leaves (48 DAS and 90 DAS) and in flowers. Jasmonate ZIM-domain protein 1 (*JAZ1*, *Solyc12g009220*) was upregulated in flowers, fruits and 48 DAS leaves and induced a gene downregulation at 90 DAS (Table 9).

With regards to salicylic acid, HMF upregulated the expression of *SAMT (Solyc00g029190)* in 48 DAS and 90 DAS leaves as well as in flowers and unripe fruits, but downregulated *SAMT* expression in ripe fruits. A gene encoding for a similar function, *O-methyltransferase* (*Solyc02g077530*), was strongly upregulated in 90 DAS leaves (Table 9).

3.9. HMF induces developmental and organ differential gene expression

A heatmap generated by combining all gene fold changes between plants exposed to HMF and GMF (HMF/GMF) clearly indicates that reducing the GMF to HMF values prompts a differential gene expression not only during leaf development, but also among the different stages of fruit development (from flowers to ripe fruits) (Fig. 6). Four major clusters are evident: cluster 1 contains the two homologs of the *D. melanogaster* magnetosensing gene MagR (*Isca-like 1* and *erpA 2*) and comprises most of the genes involved in ROS production and scavenging, evidencing a common trend between unripe fruits and leaves at 75 DAS; cluster 2 gathers genes coding for carotenoid, ABA and glutathione metabolism, and is dominated by the upregulation of these genes in ripe fruits and downregulation in flowers; cluster 3 is made by four genes, two of which (*ZEP* and *RRA2*) are strongly downregulated in flowers; finally, cluster 4 gathers all remaining genes which are characterized by the opposite trend of unripe fruits with respect to all other organs under study (Fig. 6). In developing leaves, the downregulation of *Isca-like 1* and *erpA 2* correlates with the downregulation of most of the genes under study, particularly in 75 DAS leaves. On the contrary, the regulation of many flowers, unripe and ripe fruits genes show overall opposite trends. Upregulation of *Isca-like 1* and *erpA 2* correlates with the downregulation of cluster 4 genes in flowers and ripe fruits, whereas the downregulation of the two genes correlates with the upregulation of cluster 5 unripe fruit genes (Fig. 6).

4. Discussion

The geology of our planet produces a magnetic field (GMF) that has existed since the dawn of life on Earth. Numerous studies have shown that living organisms, ranging from bacteria to mammals, respond to changes in the GMF. This suggests that magnetic fluctuations influence various species to different extents and for diverse purposes. The results of this work demonstrate that tomato is also subjected to magnetic induction, by responding to HMF differently, depending on the development stage and the organ analyzed. These results agree with previous works demonstrating the plant differential magnetic induction between diverse organs (Belyavskaya, 2004; Dziwulska-Hunek et al., 2020; Paponov et al., 2021).

MagR is a highly conserved ISCA protein that forms a rod-like complex with cryptochromes (Cry) for a putative magnetoreceptor of living organisms (Guo et al., 2018; Qin et al., 2016). By using external magnetic field stimulations, it has been shown that MagR can be regulated affecting the expression of related magnetoreceptors (Wang et al., 2016). Moreover, iron-sulfur binding as well as iron binding were demonstrated to play essential and synergistic roles in MagR magnetism. This enables MagR to achieve complex functions and diversity among species, even with highly conserved sequences (Zhang et al., 2024; Zhou et al., 2023). Two tomato MagR homologs, *Isca-like 1* and *erpA 2*, are clearly modulated by HMF, with their modulation showing either positive or negative correlations with many of the tomato genes under study. In this work we found positive correlations (i.e., same up or downregulation) with most of the leaf genes coding for phytohormones, ROS scavenging and production, and lipid metabolism whereas an almost reversed trend was found in flowers and fruits. Interestingly, the downregulation of *Isca-like 1* and *erpA 2* correlated with an upregulation of most unripe fruit gene expression (Fig. 6). From a metabolic point of view, *Isca-like 1* and *erpA 2* downregulation by HMF correlated with the reduction of chlorophyll content of leaves and unripe fruits, and the increased content of Chl precursors and catabolites. Moreover, leaf carotenoids and xanthophylls were also reduced in leaves causing a decreased photosynthetic efficiency and a decreased NPQ. Same correlations were found between *Isca-like 1* and *erpA 2* downregulation and the expression of most of the genes involved in polyphenols biosynthesis, which caused a significant reduction of leaf polyphenol content. Carotenoids quench excess excitation of Chl and reduce the formation of ROS (Rinalducci et al., 2004) while polyphenols and scavenging enzymes can effectively mitigate Chl degradation trough their ability to scavenge ROS within the chloroplasts (Wang et al., 2022). A comprehensive transcriptomic analysis of Arabidopsis plants under HMF conditions reveals that alteration of the GMF can be considered an abiotic stress (Paponov et al., 2021). Abiotic stress factors influence Chl biosynthesis, with significant implications for crop yields and economic productivity (Li et al., 2024). Our results indicate that HMF impacts on tomato photosynthesis and eventually plant productivity. It is known

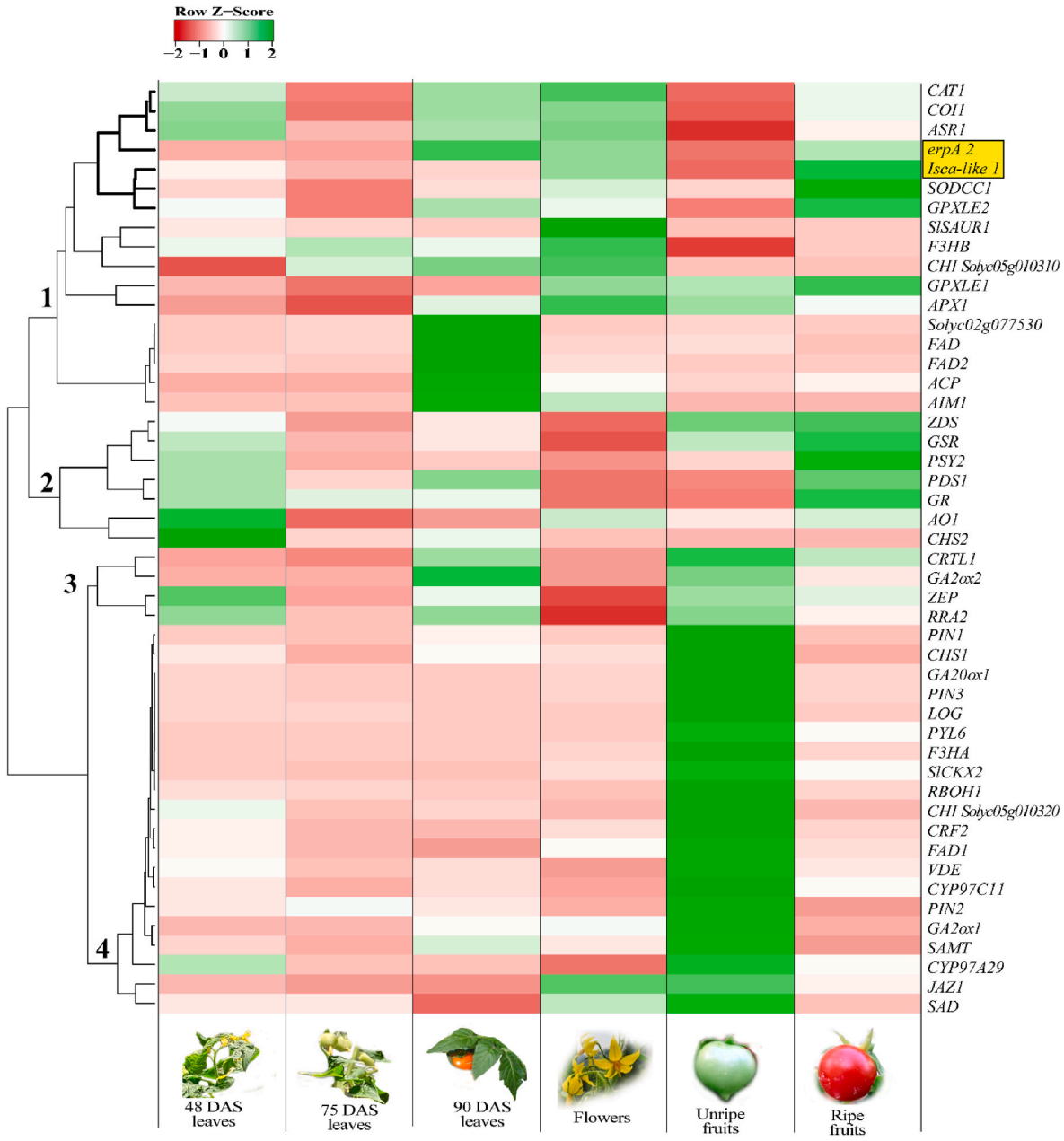

Fig. 6. Heatmap generated by considering the HMF/GMF ratio of all tomato genes considered in this work. Clustering was obtained with Pearsonian single linkage method. The yellow shading highlights the two ISCA genes of tomato homolog to the *D. melanogaster* MagR. Four main clusters are evident. (For interpretation of the references to colour in this figure legend, the reader is referred to the Web version of this article.)

that the photosynthetic machinery occurs almost exclusively in green leaves; however other vegetative and reproductive structures like green stems, green fruits, and green flower organs can be photosynthetically active (Simkin et al., 2020). HMF exposure significantly impacted unripe tomato fruits, leading to a significant reduction of Chl content. This reduction was correlated in ripe fruits with decreased levels of some carotenoids and of the bioactive compound lycopene. The overall reduction of carotenoids, polyphenols, and fatty acids, along with the increased amount of ROS of tomato ripe fruit, indicates that HMF lowers the quality of tomato production. This could pose a critical challenge for specific environments such as space farming.

The reduction of H_2O_2 in leaves at 48 and 75 DAS leaves was closely correlated with a decrease in total Chl content than with an increase of the scavenging systems activity. In contrast, in flowers and fruits, the increased H_2O_2 levels were associated to increased expression of genes coding for ROS-producing enzymes (e.g., *RBOH1*). These results are in line with the general concept that HMF can influence the production of ROS, alters the normal signaling roles of these reactive species and regulates physiological processes at the cellular level (Zhang and Tian, 2020). Indeed, alteration of the GMF affects ROS production (Wang and Zhang, 2017) and interferes with the transcription of ROS scavenging systems (Parmagnani et al., 2022b).

ISCAs expression closely mirrors the expression of genes coding for phytohormone regulation. In particular, modulation of ISCAs correlates with the expression of genes coding for auxin transport, as well as for the small auxin up-regulated RNA (*SlSAUR1*, *Solyc01g091030*) especially in flowers and unripe fruits. SAURs are primary auxin response genes hypothesized to be involved in auxin signaling pathways; they show an accumulating pattern of mRNA along tomato flower and fruit development and are regulated by abiotic stress (Wu et al., 2012). Upregulation of ISCA correlates with a general reduction of gibberellin content and downregulation of *GA20ox1*, (*Solyc03g006880*), that codes for a protein

involved in early steps during GA synthesis (Mignolli et al., 2015); however, a reverse correlation was found in unripe fruits where the content of both GA_1 and GA_4 as well as the expression of *GA20ox1* was increased. During tomato fruit set, cell division as well as cell elongation are finely coordinated by a balance between gibberellins and auxins. Moreover, the biosynthesis of gibberellin can be promoted by auxin, while other growth regulators, such as ethylene, abscisic acid and cytokinin may also play an important role (de Jong et al., 2009). ISCA expression was also found to correlate with cytokinins metabolism. While there was no effect of HMF on *trans*-zeatin, the two precursors: zeatin riboside (Zr) and isopentenyl adenine (iP), were differentially modulated. Upregulation of ISCA correlates with the downregulation of *LOG* (*Solyc09g007830*), that codes for a cytokinin riboside 5′-monophosphate phosphoribohydrolase, which converts into active free bases inactive cytokinin nucleotides (Kuroha et al., 2009). However, no correlation was found with cytokinin oxidase 2 (*SlCKX2*), which encodes for a cytokinin-deactivating enzyme (Werner et al., 2001) and is a hormone-regulated gene induced by cytokinin. The aldehyde oxidase gene family is known to be the catalysts of the last step in the biosynthesis of indole-3-acetic acid (IAA, auxin) and also of abscisic acid (ABA) in tomato (Min et al., 2000). ISCA upregulation correlated with aldehyde oxidase 1 (*AO1*, *Solyc11g071620*) downregulation that reduced the amount of ABA. As a consequence, *PYL6* (*Solyc03g095780*) a pyrabactin resistance1-like protein involved in ABA perception (González-Guzmán et al., 2014), was also downregulated, in 90 DAS leaves and strongly upregulated in unripe fruits, where the two ISCA were downregualted. Tomato *AIM1* (*Solyc12g099120*) encodes the R2R3MYB protein ABA-induced MYB1, that is involved in ABA response to abiotic stresses and oxidative stress (AbuQamar et al., 2009). AIM1 expression paralleled ISCAs expression, particularly in 90 DAS leaves and in unripe fruits. The ABA stress ripening gene, *ASR1* (*Solyc04g071610*) that plays multiple roles in plant responses to abiotic stresses (Dominguez et al., 2021), was also correlated to ISCA expression as was *ZEP* (*Solyc02g090890*), encoding a zeaxanthin epoxidase (Burbidge et al., 1997) involved in ABA biosynthesis. Overall, the regulation of ABA gene expression prompted a general increase in the ABA inactivated product, ABA-GE. ABA-GE is formed in the cytoplasm and stored in the vacuoles (Chen et al., 2020), it is considered a source of stress-induced apoplastic ABA (Netting et al., 2012) and plays a potential role in root-to-shoot signaling (Sauter et al., 2002). Reduction of ABA affects fruit ripening (Kou et al., 2021) and contributes to lower tomato fruit quality under HMF condition. *COI1* (*Solyc05g052620*) encodes an F-box protein required for the expression of JA-responsive genes and in tomato is involved in reproductive development (Abdelkareem et al., 2017), whereas JAZ1 (*Solyc12g009220*) proteins are key regulators in the JA signaling pathway and function to repress the expression of JA-responsive genes (Valenzuela-Riffo et al., 2018). Both genes were co-regulated with *Isca-like 1* and *erpA 2*, with a reduction of the JA content. *SAMT* (*Solyc00g029190*) and *O-methyltransferase* (*Solyc02g077530*) encode for an *S*-adenosyl-L-methionine salicylic acid carboxyl methyltransferase that catalyzes the formation of methyl salicylate from salicylic acid and *S*-adenosyl-L-methionine (Tieman et al., 2010). *SAMT* showed the same pattern expression of the two tomato ISCA, whereas *O-methyltransferase* was only upregulated in 90 DAS leaves. ABA, JA, SA and GAs play important roles in modulating secondary plant products being involved in transport, synthesis and site of production (Lv et al., 2021). The interplay among phytohormones and their influence on tomato secondary metabolites (polyphenols)

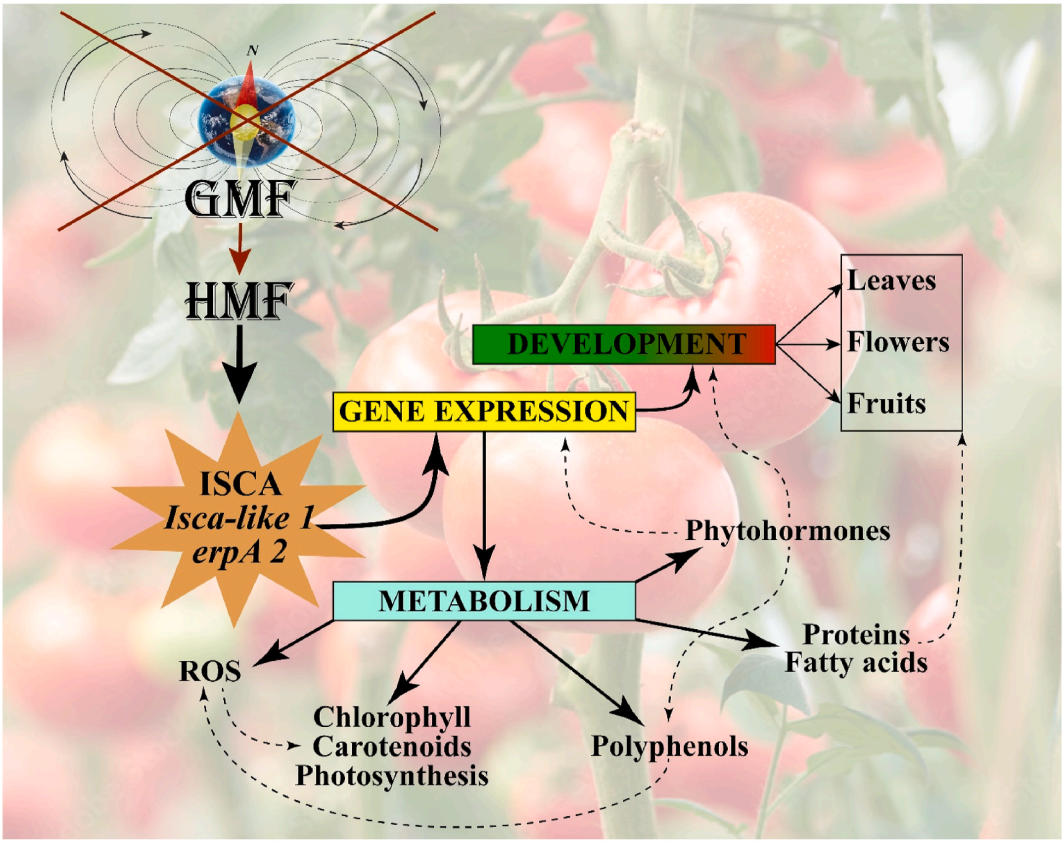

Fig. 7. Working hypothesis for the potential interaction between tomato ISCA and tomato gene expression, metabolism and development. The reduction of the geomagnetic field (GMF) to hypomagnetic values (HMF) modulates the tomato homolog of the MagR magnetosensors *Isca-like 1* and *erpA 2*. The differential expression of these genes is associated to the modulation of the expression of genes coding for primary and secondary metabolites, including ROS, proteins, fatty acids, polyphenols, chlorophylls, carotenoids and phytohormones. Solid line indicates putative direct effects on gene expression or production of molecules, dotted lines indicate potential cross-talks.

production as well as the overlapping of gene expressions among genes coding for these metabolites and the tomato ISCAs under study suggest an important role of MagR homologs in tomato responses to HMF.

In conclusion, our working hypothesis is that the modulation of tomato homologs of the magnetoreceptor MagR, *Isca-like 1* and *erpA 2*, by the environmental magnetic might be associated with the observed modulation of different genes coding for some proteins involved in plant development and metabolism (Fig. 7).

Besides considerations on the important role of the GMF on plant evolution (see for instance Maffei (2014)), the finding that HMF reduces tomato fruit quality is of major importance for space farming. Future space missions and habitats will likely include agricultural production systems designed to provide fresh and nutritious foods to the crew's diet (Maffei et al., 2024; Paul et al., 2022). Moreover, long-term space exploration necessitates the utilization of plant-based materials not solely for food production, but also for medicines, to enhance mental well-being of astronauts and repair compounds, such as plastics, among others (Viejo et al., 2024). Beyond Low Earth Orbit (LEO), besides radiation and pressure, nothing is still known on the effects of the absence of a GMF. The results presented show that tomato fruit quality will be potentially reduced beyond LEO, thus threatening the quality of food production. The results of this work confirm our previous observations on Arabidopsis, maize and beans with a general reduction of crop productivity under HMF conditions. Therefore, a major effort is required to better understand the nature of plant magnetoreception to sustain plant productivity both in space beyond LEO and on Earth.

The ongoing research focuses on the two ISCA genes identified in this study as well as other ISCA that may play a role in tomato magnetoreception by using CRISPR-Cas9 editing followed by mRNA-Seq of mutants and wild type plants and the results will be reported soon.

CRediT authorship contribution statement

Giuseppe Mannino: Writing – review & editing, Methodology, Investigation, Formal analysis, Data curation, Conceptualization. **Ambra S. Parmagnani:** Writing – review & editing, Methodology, Investigation, Formal analysis. **Massimo E. Maffei:** Writing – original draft, Visualization, Validation, Supervision, Resources, Project administration, Methodology, Investigation, Funding acquisition, Formal analysis, Data curation, Conceptualization.

Declaration of competing interest

The authors declare that they have no known competing financial interests or personal relationships that could have appeared to influence the work reported in this paper.

Acknowledgments

The work was funded by the PRIN2022 project TREESMAG (2022ENLMBY).

Appendix A. Supplementary data

Supplementary data to this article can be found online at https://doi.org/10.1016/j.jplph.2025.154453.

Data availability

Data will be made available on request.

References

Abdelkareem, A., Thagun, C., Nakayasu, M., Mizutani, M., Hashimoto, T., Shoji, T., 2017. Jasmonate-induced biosynthesis of steroidal glycoalkaloids depends on COI1 proteins in tomato. Biochem. Biophys. Res. Commun. 489 (2), 206–210.

Abir, M.H., Mahamud, A., Tonny, S.H., Anu, M.S., Hossain, K.H.S., Protic, I.A., Khan, M. S.U., Baroi, A., Moni, A., Uddin, M.J., 2023. Pharmacological potentials of lycopene against aging and aging-related disorders: a review. Food Sci. Nutr. 11 (10), 5701–5735.

AbuQamar, S., Luo, H.L., Laluk, K., Mickelbart, M.V., Mengiste, T., 2009. Crosstalk between biotic and abiotic stress responses in tomato is mediated by the *AIM1* transcription factor. Plant J. 58 (2), 347–360.

Ageeb, G.W., Talaab, A.S., Abd El-Hady, M., Eldardiry, E.I., Wahab, M.A.M., 2018. The impact of magnetized saline irrigation water treatment on soil, water and plant. Biosci. Res. 15 (4), 4106–4112.

Agliassa, C., Maffei, M.E., 2019. Reduction of geomagnetic field (GMF) to near null magnetic field (NNMF) affects some *Arabidopsis thaliana* clock genes amplitude in a light independent manner. J. Plant Physiol. 232 (1), 23–26.

Agliassa, C., Narayana, R., Bertea, C.M., Rodgers, C.T., Maffei, M.E., 2018a. Reduction of the geomagnetic field delays *Arabidopsis thaliana* flowering time through downregulation of flowering-related genes. Bioelectromagnetics 39 (5), 361–374.

Agliassa, C., Narayana, R., Christie, J.M., Maffei, M.E., 2018b. Geomagnetic field impacts on cryptochrome and phytochrome signaling. J. Photochem. Photobiol. B Biol. 185 (8), 32–40.

Babicki, S., Arndt, D., Marcu, A., Liang, Y., Grant, J.R., Maciejewski, A., Wishart, D.S., 2016. Heatmapper: web-enabled heat mapping for all. Nucleic acids research 44 (W1), W147–W153.

Babu, M.A., Srinivasan, R., Subramanian, P., Kodiveri Muthukaliannan, G., 2020. RNAi silenced ζ-carotene desaturase developed variegated tomato transformants with increased phytoene content. Plant Growth Regul. 93 (2), 189–201.

Belyavskaya, N.A., 2004. Biological effects due to weak magnetic field on plants. Adv. Space Res. 34 (7), 1566–1574.

Bourget, S., Corcuff, R., Angers, P., Arul, J., 2011. Effect of the exposure to static magnetic field on the ripening and senescence of tomato fruits. In: 4th International Conference on Postharvest Unlimited. Int Soc Horticultural Science. WA, Leavenworth, pp. 129–133.

Burbidge, A., Grieve, T., Terry, C., Corlett, J., Thompson, A., Taylor, I., 1997. Structure and expression of a cDNA encoding zeaxanthin epoxidase, isolated from a wilt-related tomato (Lycopersicon esculentum Mill.) library. J. Exp. Bot. 48 (314), 1749–1750.

Cecchin, M., Cazzaniga, S., Martini, F., Paltrinieri, S., Bossi, S., Maffei, M.E., Ballottari, M., 2022. Astaxanthin and eicosapentaenoic acid production by S4, a new mutant strain of *Nannochloropsis gaditana*. Microb. Cell. Fact. 21 (1), 15.

Chen, T.T., Liu, F.F., Xiao, D.W., Jiang, X.Y., Li, P., Zhao, S.M., Hou, B.K., Li, Y.J., 2020. The Arabidopsis UDP-glycosyltransferase75B1, conjugates abscisic acid and affects plant response to abiotic stresses. Plant Mol. Biol. 102 (4–5), 389–401.

de Jong, M., Mariani, C., Vriezen, W.H., 2009. The role of auxin and gibberellin in tomato fruit set. J. Exp. Bot. 60 (5), 1523–1532.

De Souza-Torres, A., Sueiro-Pelegrin, L., Zambrano-Reyes, M., Macias-Socarras, I., Gonzalez-Posada, M., Garcia-Fernandez, D., 2020. Extremely low frequency non-uniform magnetic fields induce changes in water relations, photosynthesis and tomato plant growth. Int. J. Radiat. Biol. 96 (7), 951–957.

de Souza, A., García, D., Sueiro, L., Gilart, F., Porras, E., Licea, L., 2006. Pre-sowing magnetic treatments of tomato seeds increase the growth and yield of plants. Bioelectromagnetics 27 (4), 247–257.

Depège, N., Drevet, J., Boyer, N., 1998. Molecular cloning and characterization of tomato cDNAs encoding glutathione peroxidase-like proteins. Eur. J. Biochem. 253 (2), 445–451.

Dhiman, S.K., Galland, P., 2018. Effects of weak static magnetic fields on the gene expression of seedlings of Arabidopsis thaliana. J. Plant Physiol. 231 (9), 9–18.

Dominguez, P.G., Conti, G., Duffy, T., Insani, M., Alseekh, S., Asurmendi, S., Fernie, A.R., Carrari, F., 2021. Multiomics analyses reveal the roles of the ASR1 transcription factor in tomato fruits. J. Exp. Bot. 72 (18), 6490–6509.

Dziwulska-Hunek, A., Kornarzynska-Gregorowicz, A., Niemczynowicz, A., Matwijczuk, A., 2020. Influence of electromagnetic stimulation of seeds on the photosynthetic indicators in medicago sativa L. Leaves at various stages of development. Agronomy-Basel 10 (4), 17.

Fattore, M., Montesano, D., Pagano, E., Teta, R., Borrelli, F., Mangoni, A., Seccia, S., Albrizio, S., 2016. Carotenoid and flavonoid profile and antioxidant activity in "Pomodorino Vesuviano" tomatoes. J. Food Compos. Anal. 53 (10), 61–68.

Fiorillo, A., Parmagnani, A.S., Visconti, S., Mannino, G., Camoni, L., Maffei, M.E., 2023. 14-3-3 proteins and the plasma membrane H(+)-ATPase are involved in maize (Zea mays) magnetic induction. Plants 12 (15), 2887.

Fraser, P.D., Schuch, W., Bramley, P.M., 2000. Phytoene synthase from tomato (*Lycopersicon esculentum*) chloroplasts -: partial purification and biochemical properties. Planta 211 (3), 361–369.

Friml, J., Wiśniewska, J., Benková, E., Mendgen, K., Palme, K., 2002. Lateral relocation of auxin efflux regulator PIN3 mediates tropism in Arabidopsis. Nature 415 (6873), 806–809.

González-Guzmán, M., Rodríguez, L., Lorenzo-Orts, L., Pons, C., Sarrión-Perdigones, A., Fernández, M.A., Peirats-Llobet, M., Forment, J., Moreno-Alvero, M., Cutler, S.R., Albert, A., Granell, A., Rodríguez, P.L., 2014. Tomato PYR/PYL/RCAR abscisic acid receptors show high expression in root, differential sensitivity to the abscisic acid agonist quinabactin, and the capability to enhance plant drought resistance. J. Exp. Bot. 65 (15), 4451–4464.

Guo, J.P., Wan, H.Y., Matysik, J., Wang, X.J., 2018. Recent advances in magnetosensing cryptochrome model systems. Acta Chim. Sin. 76 (8), 597–604.

Han, H., Gao, S., Li, B., Dong, X.C., Feng, H.L., Meng, Q.W., 2010. Overexpression of violaxanthin de-epoxidase gene alleviates photoinhibition of PSII and PSI in tomato during high light and chilling stress. J. Plant Physiol. 167 (3), 176–183.

Jegadeesan, S., Chaturvedi, P., Ghatak, A., Pressman, E., Meir, S., Faigenboim, A., Rutley, N., Beery, A., Harel, A., Weckwerth, W., Firon, N., 2018. Proteomics of heat-stress and ethylene-mediated thermotolerance mechanisms in tomato pollen grains. Front. Plant Sci. 9 (11), 20.
Kawasaki, T., Koeduka, T., Sugiyama, A., Sasaki, K., Linley, P.J., Shitan, N., Kumano, T., Yamamoto, H., Ezura, H., Kuzuyama, T., Yazaki, K., 2014. Metabolic engineering of flavonoids with prenyltransferase and chalcone isomerase genes in tomato fruits. Plant Biotechnol. 31 (5), 567–571.
Kharshiing, E.V., Kumar, G.P., Ditengou, F.A., Li, X., Palme, K., Sharma, R., 2010. The *polycotyledon (pct1-2*) mutant of tomato shows enhanced accumulation of PIN1 auxin transport facilitator protein. Plant Biol 12 (1), 224–228.
Kou, X.H., Yang, S., Chai, L.P., Wu, C.E., Zhou, J.Q., Liu, Y.F., Xue, Z.H., 2021. Abscisic acid and fruit ripening: multifaceted analysis of the effect of abscisic acid on fleshy fruit ripening. Sci. Hortic. 281 (4), 11.
Kumar, M., Ahuja, S., Dahuja, A., Kumar, R., Singh, B., 2014. Gamma radiation protects fruit quality in tomato by inhibiting the production of reactive oxygen species (ROS) and ethylene. J. Radioanal. Nucl. Chem. 301 (3), 871–880.
Kuroha, T., Tokunaga, H., Kojima, M., Ueda, N., Ishida, T., Nagawa, S., Fukuda, H., Sugimoto, K., Sakakibara, H., 2009. Functional analyses of LONELY GUY cytokinin-activating enzymes reveal the importance of the direct activation pathway in Arabidopsis. Plant Cell 21 (10), 3152–3169.
Li, X., Zhang, W., Niu, D., Liu, X., 2024. Effects of abiotic stress on chlorophyll metabolism. Plant science : an international journal of experimental plant biology 342 (5), 112030.
Lv, Z.Y., Sun, W.J., Jiang, R., Chen, J.F., Ying, X., Zhang, L., Chen, W.S., 2021. Phytohormones jasmonic acid, salicylic acid, gibberellins, and abscisic acid are key mediators of plant secondary metabolites. World J. Trad. Chinese Med. 7 (3), 307–325.
Maffei, M.E., 2014. Magnetic field effects on plant growth, development, and evolution. Front. Plant Sci. 5, 15.
Maffei, M.E., 2022. Magnetoreception in plants. In: Shoogo, U., Tsukasa, S. (Eds.), Bioelectromagnetism. History, Foundations and Applications. CRC Press, Boca Raton, FL, U.S.A., pp. 191–214
Maffei, M.E., Balestrini, R., Costantino, P., Lanfranco, L., Morgante, M., Battistelli, A., Del Bianco, M., 2024. The physiology of plants in the context of space exploration. Commun. Biol. 7 (1), 1311.
Matsuo, S., Kikuchi, K., Fukuda, M., Honda, I., Imanishi, S., 2012. Roles and regulation of cytokinins in tomato fruit development. J. Exp. Bot. 63 (15), 5569–5579.
Meng, C., Zhang, S., Deng, Y.S., Wang, G.D., Kong, F.Y., 2015. Overexpression of a tomato flavanone 3-hydroxylase-like protein gene improves chilling tolerance in tobacco. Plant Physiol. Biochem. 96 (11), 388–400.
Mignolli, F., Vidoz, M.L., Mariotti, L., Lombardi, L., Picciarelli, P., 2015. Induction of gibberellin 20-oxidases and repression of gibberellin 2β-oxidases in unfertilized ovaries of *entire* tomato mutant, leads to accumulation of active gibberellins and parthenocarpic fruit formation. Plant Growth Regul. 75 (2), 415–425.
Min, X.J., Okada, K., Brockmann, B., Koshiba, T., Kamiya, Y., 2000. Molecular cloning and expression patterns of three putative functional aldehyde oxidase genes and isolation of two aldehyde oxidase pseudogenes in tomato. Biochim. Biophys. Acta, Gene Struct. Expression 1493 (3), 337–341.
Nakamura, S., Hondo, K., Kawara, T., Okazaki, Y., Saito, K., Kobayashi, K., Yaeno, T., Yamaoka, N., Nishiguchi, M., 2016. Conferring high-temperature tolerance to nontransgenic tomato scions using graft transmission of RNA silencing of the fatty acid desaturase gene. Plant Biotechnol. J. 14 (2), 783–790.
Netting, A.G., Theobald, J.C., Dodd, I.C., 2012. Xylem sap collection and extraction methodologies to determine *in vivo* concentrations of ABA and its bound forms by gas chromatography-mass spectrometry (GC-MS). Plant Methods 8, 14.
Nießner, C., Denzau, S., Peichl, L., Wiltschko, W., Wiltschko, R., 2014. Magnetoreception in birds: I. Immunohistochemical studies concerning the cryptochrome cycle. J. Exp. Biol. 217 (Pt 23), 4221–4224.
Noctor, G., Foyer, C.H., 1998. Ascorbate and glutathione: keeping active oxygen under control. Annu. Rev. Plant Physiol. Plant Mol. Biol. 49 (1), 249–279.
Oneill, S.D., Tong, Y., Sporlein, B., Forkmann, G., Yoder, J.I., 1990. Molecular genetic-analysis of chalcone synthase in *Lycopersicon esculentum* and an anthocyanin-deficient mutant. Mol. Gen. Genet. 224 (2), 279–288.
Paponov, I.A., Fliegmann, J., Narayana, R., Maffei, M.E., 2021. Differential root and shoot magnetoresponses in Arabidopsis thaliana. Sci. Rep. 11 (1), 9195.
Parmagnani, A.S., Betterle, N., Mannino, G., D'Alessandro, S., Nocito, F.F., Ljumovic, K., Vigani, G., Ballottari, M., Maffei, M.E., 2023. The geomagnetic field (GMF) is required for Lima bean photosynthesis and reactive oxygen species production. Int. J. Mol. Sci. 24 (3), 2896.
Parmagnani, A.S., D'Alessandro, S., Maffei, M.E., 2022a. Iron-sulfur complex assembly: potential players of magnetic induction in plants. Plant Sci. 325, 111483.
Parmagnani, A.S., Mannino, G., Maffei, M.E., 2022b. Transcriptomics and metabolomics of reactive oxygen species modulation in near-null magnetic field-induced Arabidopsis thaliana. Biomolecules 12 (12), 1824.
Patel, A.H., Sharma, H.P., Vaishali, 2023. Physiological functions, pharmacological aspects and nutritional importance of green tomato- a future food. Crit. Rev. Food Sci. Nutr. 6, 1–29.
Paul, A.L., Elardo, S.M., Ferl, R., 2022. Plants grown in Apollo lunar regolith present stress-associated transcriptomes that inform prospects for lunar exploration. Commun. Biol. 5 (1), 382.
Pecker, I., Chamovitz, D., Linden, H., Sandmann, G., Hirschberg, J., 1992. A single polypeptide catalyzing the conversion of phytoene to zeta-carotene is transcriptionally regulated during tomato fruit ripening. Proc. Natl. Acad. Sci. U. S. A. 89 (11), 4962–4966.
Perltreves, R., Galun, E., 1991. The tomato cu,zn superoxide-dismutase genes are developmentally regulated and respond to light and stress. Plant Mol. Biol. 17 (4), 745–760.
Piccolo, V., Pastore, A., Maisto, M., Keivani, N., Tenore, G.C., Stornaiuolo, M., Summa, V., 2024. Agri-food waste recycling for healthy remedies: biomedical potential of nutraceuticals from unripe tomatoes (*Solanum lycopersicum* L.). Foods 13 (2), 21.
Poinapen, D., Brown, D.C.W., Beeharry, G.K., 2013. Seed orientation and magnetic field strength have more influence on tomato seed performance than relative humidity and duration of exposure to non-uniform static magnetic fields. J. Plant Physiol. 170 (14), 1251–1258.
Pooam, M., Arthaut, L.D., Burdick, D., Link, J., Martino, C.F., Ahmad, M., 2019. Magnetic sensitivity mediated by the Arabidopsis blue-light receptor cryptochrome occurs during flavin reoxidation in the dark. Planta 249 (2), 319–332.
Pumilia, G., Cichon, M.J., Cooperstone, J.L., Giuffrida, D., Dugo, G., Schwartz, S.J., 2014. Changes in chlorophylls, chlorophyll degradation products and lutein in pistachio kernels (*Pistacia vera* L.) during roasting. Food Res. Int. 65, 193–198.
Qin, S., Yin, H., Yang, C., Dou, Y., Liu, Z., Zhang, P., Yu, H., Huang, Y., Feng, J., Hao, J., Hao, J., Deng, L., Yan, X., Dong, X., Zhao, Z., Jiang, T., Wang, H.W., Luo, S.J., Xie, C., 2016. A magnetic protein biocompass. Nat. Mater. 15 (2), 217–226.
Racuciu, M., 2019. Development of tomato (*solanum lycopersicum L.*) seedlings under the action of extremely low frequency magnetic field in a controlled environment conditions. In: 12th International Conference of Processes in Isotopes and Molecules (PIM). Amer Inst Physics, Cluj Napoca, ROMANIA.
Ralley, L., Schuch, W., Fraser, P.D., Bramley, P.M., 2016. Genetic modification of tomato with the tobacco lycopene β-cyclase gene produces high β-carotene and lycopene fruit. Z.Naturforsch.(C) 71 (9–10), 295–301.
Rinalducci, S., Pedersen, J.Z., Zolla, L., 2004. Formation of radicals from singlet oxygen produced during photoinhibition of isolated light-harvesting proteins of photosystem II. Biochim. Biophys. Acta Bioenerg. 1608 (1), 63–73.
Salem, M.A., Yoshida, T., Perez de Souza, L., Alseekh, S., Bajdzienko, K., Fernie, A.R., Giavalisco, P., 2020. An improved extraction method enables the comprehensive analysis of lipids, proteins, metabolites and phytohormones from a single sample of leaf tissue under water-deficit stress. Plant J. 103 (4), 1614–1632.
Samarah, N.H., Hani, M., Makhadmeh, I.M., 2021. Effect of magnetic treatment of water or seeds on germination and productivity of tomato plants under salinity stress. Horticulturae 7 (8), 11.
Sauter, A., Dietz, K.J., Hartung, W., 2002. A possible stress physiological role of abscisic acid conjugates in root-to-shoot signalling. Plant Cell Environ. 25 (2), 223–228.
Scandiffio, R., Bonzano, S., Cottone, E., Shrestha, S., Bossi, S., De Marchis, S., Maffei, M. E., Bovolin, P., 2023. Beta-caryophyllene modifies intracellular lipid composition in a cell model of hepatic steatosis by acting through CB2 and PPAR receptors. Int. J. Mol. Sci. 24 (7), 6060.
Schrager-Lavelle, A., Gath, N.N., Devisetty, U.K., Carrera, E., López-Díaz, I., Blázquez, M. A., Maloof, J.N., 2019. The role of a class III gibberellin 2-oxidase in tomato internode elongation. Plant J. 97 (3), 603–615.
Shi, X.L., Gupta, S., Rashotte, A.M., 2012. *Solanum lycopersicum cytokinin response factor* (*SlCRF*) genes: characterization of CRF domain-containing ERF genes in tomato. J. Exp. Bot. 63 (2), 973–982.
Simkin, A.J., Faralli, M., Ramamoorthy, S., Lawson, T., 2020. Photosynthesis in non-foliar tissues: implications for yield. Plant J. 101 (4), 1001–1015.
Soydam Aydin, S., Büyük, I., Gökçe Gündüzer, E., Büyük, B.P., Kandemir, I., Cansaran-Duman, D., Aras, S., 2016. Effects of lead (Pb) and cadmium (Cd) elements on lipid peroxidation, catalase enzyme activity and catalase gene expression profile in tomato plants. J. Agric. Sci.-Tarim Bilim. Derg. 22 (4), 539–547.
Stigliani, A.L., Giorio, G., D'Ambrosio, C., 2011. Characterization of P450 carotenoid β- and ε-hydroxylases of tomato and transcriptional regulation of xanthophyll biosynthesis in root, leaf, petal and fruit. Plant Cell Physiol. 52 (5), 851–865.
Storniolo, C.E., Sacanella, I., Lamuela-Raventos, R.M., Moreno, J.J., 2020. Bioactive compounds of mediterranean cooked tomato sauce (sofrito) modulate intestinal epithelial cancer cell growth through oxidative stress/arachidonic acid cascade regulation. ACS Omega 5 (28), 17071–17077.
Teale, W.D., Ditengou, F.A., Dovzhenko, A.D., Li, X., Molendijk, A.M., Ruperti, B., Paponov, I., Palme, K., 2008. Auxin as a model for the integration of hormonal signal processing and transduction. Mol. Plant 1 (2), 229–237.
Tieman, D., Zeigler, M., Schmelz, E., Taylor, M.G., Rushing, S., Jones, J.B., Klee, H.J., 2010. Functional analysis of a tomato salicylic acid methyl transferase and its role in synthesis of the flavor volatile methyl salicylate. Plant J. 62 (1), 113–123.
Valenzuela-Riffo, F., Garrido-Bigotes, A., Figueroa, P.M., Morales-Quintana, L., Figueroa, C.R., 2018. Structural analysis of the woodland strawberry COI1-JAZ1 co-receptor for the plant hormone jasmonoyl-isoleucine. J. Mol. Graph. 85 (10), 250–261.
Viejo, C.G., Harris, N., Fuentes, S., 2024. Assessment of changes in sensory perception, biometrics and emotional response for space exploration by simulating microgravity positions. Food Res. Int. 175, 9.
Villani, M.E., Massa, S., Lopresto, V., Pinto, R., Salzano, A.M., Scaloni, A., Benvenuto, E., Desiderio, A., 2017. Effects of high-intensity static magnetic fields on a root-based bioreactor system for space applications. Life Sci. Space Res. 15 (11), 79–87.
Wang, H.X., Xiang, Y.C., Zhang, Y.G., 2016. The proceedings of IscA that functions as a biomagnetic receptor protein (MagR). Prog. Biochem. Biophys. 43 (12), 1115–1128.
Wang, H.Z., Zhang, X., 2017. Magnetic fields and reactive oxygen species. Int. J. Mol. Sci. 18 (10), 20.
Wang, J., Chen, G., Li, X., Fu, X., Li, S., Tao, X., Chen, Z.-H., Xu, S., 2022. Transcriptome and metabolome analysis of a late-senescent vegetable soybean during seed development provides new insights into degradation of chlorophyll. Antioxidants 11 (12), 2480.

Werner, T., Motyka, V., Strnad, M., Schmülling, T., 2001. Regulation of plant growth by cytokinin. Proc. Natl. Acad. Sci. USA 98 (18), 10487–10492.
Wu, J., Liu, S.Y., He, Y.J., Guan, X.Y., Zhu, X.F., Cheng, L., Wang, J., Lu, G., 2012. Genome-wide analysis of SAUR gene family in Solanaceae species. Gene 509 (1), 38–50.
Xu, C.X., Wei, S.F., Lu, Y., Zhang, Y.X., Chen, C.F., Song, T., 2013. Removal of the local geomagnetic field affects reproductive growth in Arabidopsis. Bioelectromagnetics 34 (6), 437–442.
Xu, J.W., Kang, Z., Zhu, K.Y., Zhao, D.K., Yuan, Y.J., Yang, S.C., Zhen, W.T., Hu, X.H., 2021. *RBOH1*-dependent H_2O_2 mediates spermine-induced antioxidant enzyme system to enhance tomato seedling tolerance to salinity-alkalinity stress. Plant Physiol. Biochem. 164 (7), 237–246.
Yang, Z., Zhang, L., Zhao, S.S., Luo, N., Deng, Q.J., 2020. Comparison study of static and alternating magnetic field treatments on the quality preservation effect of cherry tomato at low temperature. J. Food Process. Eng. 43 (9), 10.
Yong, K.T., Yong, P.H., Ng, Z.X., 2023. Tomato and human health: a perspective from post-harvest processing, nutrient bio-accessibility, and pharmacological interaction. Food Frontiers 4 (4), 1702–1719.
Zhang, B.F., Tian, L.X., 2020. Reactive oxygen species: potential regulatory molecules in response to hypomagnetic field exposure. Bioelectromagnetics 41 (8), 573–580.
Zhang, J., Chang, Y.F., Zhang, P., Zhang, Y.Q., Wei, M.K., Han, C.Y., Wang, S., Lu, H.M., Cai, T.T., Xie, C., 2024. On the evolutionary trail of MagRs. Zool. Res. 45 (4), 821–830.
Zhou, Y., Yu, H., Tang, Y., Chen, R., Luo, J., Shi, C., Tang, S., Li, X., Shen, X., Chen, R., Zhang, Y., Lu, Y., Ye, Z., Guo, L., Ouyang, B., 2022. Critical roles of mitochondrial fatty acid synthesis in tomato development and environmental response. Plant physiology 190 (1), 576–591.
Zhou, Y.J., Tong, T.Y., Wei, M.K., Zhang, P., Fei, F., Zhou, X.J., Guo, Z., Zhang, J., Xu, H. T., Zhang, L., Wang, S., Wang, J.F., Cai, T.T., Zhang, X., Xie, C., 2023. Towards magnetism in pigeon MagR: iron- and iron- sulfur binding work indispensably and synergistically. Zool. Res. 44 (1), 142–152.
Zou, L.P., Li, H.X., Ouyang, B., Zhang, J.H., Ye, Z.B., 2005. Molecular cloning, expression and mapping analysis of a novel cytosolic ascorbate peroxidase gene from tomato. DNA Seq 16 (6), 456–461.